Soil CO_2 Gas Concentrations and Emissions at Kilauea Volcano, Hawaii

by

Michael K. O'Keeffe

Thesis
Submitted in Partial Fulfillment of the Requirements
for the Degree of Master's of Science in Geology

New Mexico Institute of Mining and Technology
Socorro, New Mexico

September, 1994

Abstract

Recent investigations at Mount Etna and Vulcano Island have shown that a significant portion of CO_2 gas is emitted around the flanks of volcanoes as well as through their active craters and fumaroles. The objective of this study was to measure soil CO_2 emissions within Kilauea caldera and across the Southwest Rift Zone (SRZ) in order to locate and quantify the magnitude of magmatic CO_2 emitted through soils in the area. Two methods were employed to measure soil gas CO_2 concentrations (SGCC) and soil gas CO_2 flux (SGCF). A soil probe was inserted into the soil to measure SGCC at depth and SGCF measurements were performed, using the accumulator flux chamber method, along nine transects in the SRZ and two areas within Kilauea caldera. Soil samples and gas samples were collected for analysis of microbial activity and carbon isotopic ratios.

Standard flux measurements were taken at two locations about a meter apart over the study period in order to deduce the reproducibility of the method. These standard flux measurements varied at the same site day to day and from place to place probably due to meteorological factors. The most important factors effecting both SGCC and SGCF are rain and wind, but due to the great meteorological variations present across Kilauea, this could not be confirmed. One other important factor when performing these measurements at Kilauea is the limited existence of soil and the existence of cracks which provide channelways for gas escape. The calculated standard deviation is $\pm 35\%$ to $\pm 53\%$ for all SGCF measurements. In general, the slopes of soil CO_2 emissions over time were highly linear using the accumulator method.

The source of CO_2 emitted from the soil was deduced using carbon isotopic analysis and microbial activity analysis. The organic CO_2 contribution was found to be negligible in the area while a direct correlation between higher $\delta^{13}C$ (>-5 per mil) values and higher CO_2 flux suggests a magmatic source for most of the soil CO_2 gas. SGCC around Halemaumau and the SRZ are relatively high (>500 ppm CO_2) in most places at depths ranging from 5 to 85 cm. The proximity to cracks with visible steam sometimes correlated with higher soil CO_2 concentrations. When the SGCCs were compared with SGCF measurements, higher soil CO_2 concentrations (350-3000 ppm CO_2) at depth did not indicate higher CO_2 flux at the surface.

SGCF along the SRZ are much lower than those within Kilauea caldera. This suggests that most CO_2 degassed by Kilauea enters the atmosphere within the caldera. After averaging soil CO_2 fluxes across a 0.414 km^2 area, it was assumed that this area has similar soil CO_2 degassing and was representative of the area of the caldera (about 11 km^2). The entire caldera is calculated to emit about 2,300 ($\pm 35\%$ to $\pm 53\%$) Mg CO_2/day from soil emissions alone. Using a CO_2/SO_2 ratio of 9 and SO_2 COSPEC data, it is calculated that Halemaumau emits about 783 to 2367 Mg CO_2/day. Therefore, Kilauea caldera emits as much CO_2 from its soils than from active vents. The combined total estimated flux for Kilauea caldera ranges from 3100 to 4700 Mg CO_2/day which contributes a small amount (0.9%) of CO_2 compared to the total CO_2 output by global volcanism.

Acknowledgements

The author would like to express his gratitude to all the people and organizations that made this possible. This work was supported by a research grant from the New Mexico Tech Research Committee and the New Mexico Tech Graduate Office. I would like to thank my advisor Dr. Philip Kyle for supporting this research project and for his patience and time. Thanks goes to the rest of my committee; Dr. Nelia Dunbar, for her ideas and prompt review; Dr. Andrew Campbell, for his ideas, analysis of gas samples and prompt review. The staff at the Hawaiian Volcanic Observatory, especially Dr. Jeff Sutton and Tamar Elias, helped in providing access to the study area and with logistics. Thanks goes to Dr. Mike Reimer at the USGS in Denver, for his suggestions and knowledge of soil gases. I would also like to thank Ellen Wilch and Dr. Tom Kieft for analyzing the microbial activity in my soil samples; and Richard Esser for his assistance in the field.

I am indebted to my parents and family for their moral and financial support. I would also like to thank Big Ed Fry, Terry the Pollock and Scottie Douglas for their help with semi-voluntary sanity ejections.

Table of Contents

List of Figures

List of Tables

Introduction

Magmatic gasses play a fundamental role in propelling magma to the Earth's surface, and controlling explosive volcanic eruptions. Magmatic gas solubility is roughly proportional to the partial pressure of the free gas phase in equilibrium with the melt (Tazieff, 1983), or essentially to the pressure at which the magma resides. Under high pressures, magmatic volatiles are dissolved but under low pressures, when a magma rises towards the surface, the volatiles exsolve forming a vapor phase (Tazieff, 1983). Rapid exsolution of a vapor phase can cause explosive eruptions, but under other conditions the volatiles are able to rise passively through the melt and escape through a central volcanic vent. The most abundant volatile species in basaltic and andesitic magmas are H_2O (35-90 mol%), CO_2 (5-50 mol%) and SO_2 (2-30 mol%) (Anderson, 1975; Gerlach, 1982).

Volcanic carbon dioxide emissions are important in many different aspects and have been quantified by several different methods in order to: 1.) estimate the global contribution of CO_2 by volcanism (Gerlach, 1991), 2.) monitor volcanic activity and forecast volcanic events (Harris et al., 1981), 3.) deduce subsurface magma volumes and, 4.) better our understanding of volcanic evolution (Gerlach and Graeber, 1985; Greenland et al., 1985). Measurements of CO_2 emissions have been made from: 1.) active fumaroles, 2.) direct measurement in the plume by a infrared spectrophotometer mounted on an aircraft and 3.) indirect measurements by remote sensing of crater plumes using COSPEC (correlation spectrometry) SO_2 measurements and carbon/sulfur (C/S) ratios measured in active fumaroles.

Recent investigations on Mount Etna, Sicily, and Vulcano Island, Italy, have

shown that a significant portion of magmatically derived CO_2 gas is emitted around the flanks of volcanoes as well as through their active craters and fumaroles (Baubron et al., 1990; Allard, 1991). Baubron et al. (1990) estimated that 30 Mg (Megagrams) CO_2 per day ($\pm$ 20%) is emitted from soil degassing over the entire exposed surface of the Fossa cone, Vulcano, excluding fumarolic fields. These diffuse soil emanations account for about 15% of the total (180 Mg CO_2/d) CO_2 flux during Vulcano's non-eruptive stage (Baubron et al., 1990). Baubron et al. (1991) also found diffuse soil gas release at several volcanoes in quiescent stages, including Vesuvius and Solfatara (Italy), Soufriere (Guadeloupe), Lamongan and Dieng (Indonesia).

Allard et al. (1991) measured eruptive and diffuse emissions of magmatic CO_2 from Mount Etna. Their soil gas data provided evidence of CO_2 being emitted from the flanks of Etna, the amount decreasing with greater distance from active fumaroles and craters. Etna releases about 70,000 Mg of CO_2 per day (Mg/d) from its crater and approximately 55,000 Mg CO_2/d ($\pm$ 30%) from diffuse flank emissions. They conclude that diffuse flank emissions may release as much CO_2 as summit crater degassing.

From this, it is clear that the role of flank CO_2 emissions needs to be taken into account when evaluating the CO_2 budgets of volcanoes and of total subaerial volcanism (Allard et al., 1991). If diffuse CO_2 soil emanations are produced at the volcanoes mentioned above, then it is possible that diffuse CO_2 emanations are produced at other active volcanoes. Reimer (1992) proposed, based on soil CO_2 gas flux measurements made along the SRZ, that soil CO_2 emissions make a significant

contribution in the summit area of Kilauea Volcano, Hawaii, even during quiescent episodes. He estimated that these emissions are at least equal to the total degassing from the active vents most of which occur in Halemaumau crater.

The observations summarized above suggest that CO_2 is degassed from Kilauea's flanks during non-eruptive summit conditions. It is clear that CO_2 is degassed from the summit fumaroles and from Halemaumau crater (Gerlach and Graeber, 1985; Greenland et.al., 1985; Hinkle and Stokes, 1989; and Elias et al., 1993) but other areas, such as the Southwest Rift Zone (SRZ), might emit large amounts of CO_2 gas from the soil. The latter has been previously overlooked. If Kilauea emits CO_2 from visible active fumaroles and fissures near Halemaumau, then magmatic CO_2 might also be emitted through the soils and smaller cracks over the entire area of the caldera. By quantifying the soil CO_2 emissions from the caldera and the SRZ, a comparison can be made between their magnitudes in order to better define the CO_2 degassing systematics and CO_2 budget of Kilauea volcano. The objective of this study was to measure soil CO_2 emissions within Kilauea caldera and across the SRZ in order to quantify the magnitude of magmatic CO_2 emitted from the volcano and its flanks.

Carbon Dioxide

Tholeiitic basalt magmas contain large amounts of dissolved CO_2 (Pan et al., 1991). Solubility studies reveal that CO_2 is insoluble in basaltic magma and can exsolve under 5 to 10 kilobars pressure. The solubility of CO_2 in tholeiitic melt is

dependent on pressure but independent of temperature (Stolper and Holloway, 1988; Pan et al., 1991). Carbon dioxide solubility in basaltic liquids is described by Stolper and Holloway's (1988) simplified reaction:

$$CO_{2(vapor)} + O^{2-}_{(melt)} \rightarrow CO^{2-}_{3(melt)}$$

Because of its low solubility, CO_2 probably dominates the vapor phase from mantle depths up to shallow levels depending on the initial CO_2 concentration in the melt (Anderson, 1975). This low solubility allows CO_2 to exsolve at greater depth than H_2O and SO_2, to be emitted during non-eruptive activity or before the magma reaches the surface and, therefore, to be an important precursor for eruptions (Allard, 1992).

Soil Gases

Soil gas fills spaces that are not occupied by water in the soil (Glinski and Stepniewski, 1985). In a biological sense, there are four main constituents of most soil atmospheres: N_2, O_2, Ar and CO_2 (Bremner and Blackmer, 1982) with varying degrees of water vapor (Glinski and Stepniewski, 1985). Aerobic respiration by plant roots and microorganisms account for the largest production and consumption of soil gases (Bremner and Blackmer, 1982). These aerobic respiration processes consume oxygen and produce CO_2 (Bremner and Blackmer, 1982; Anderson, 1982), thus soil air contains more CO_2 and less O_2 than atmospheric air (Glinski and Stepniewski, 1985). The CO_2 concentration of clean, dry atmospheric air near sea level is about 332 ppm (Bremner and Blackmer, 1982), but is steadily increasing due to anthropogenic production (Schneider, 1989). Globally, atmospheric CO_2

concentrations have risen about 25% since 1850, while records at Mauna Loa observatory, Hawaii show that atmospheric CO_2 concentrations have increased from about 310 to 350 ppm since 1958 (Schneider, 1989). In general, aerobic respiration can be considered a secondary process in the generation of gas anomalies, as defined by McCarthy and Reimer (1986) and discussed below, and has little importance to this study. However, one must quantify the amount of CO_2, in this case, produced by aerobic respiration in order to accurately define the origin of higher CO_2 concentrations presented in this study.

McCarthy and Reimer (1986) give an excellent review of soil gas exploration for natural resources using gases that emanate to the surface from mineral deposits. They define two processes for the generation of soil gas anomalies: primary and secondary. Primary processes include: 1.) outgassing from the mantle and deep crust and 2.) venting of volatiles through volcanically active areas. Secondary processes, like aerobic respiration, produce gas anomalies through the interaction of crustal rocks with the hydrosphere, biosphere and atmosphere (McCarthy and Reimer, 1986). In this study, we are more interested with the primary processes or venting of primary CO_2 from Kilauea Volcano.

The movement of primary gases through soils, cracks and faults is important when assessing their emission rates. According to McCarthy and Reimer (1986), there are two processes by which gas migrates through the soil: 1.) diffusion and 2.) mass transport. Diffusion within soil is primarily controlled by the character of the soil, size and molecular weight of the gas species diffusing, and the temperature of

the gas (McCarthy and Reimer, 1986). McCarthy and Reimer (1986) point out that diffusion is only a mechanism for slow transport of gases over short distances whereas mass transport, the transport of gases within a moving medium, can account for rapid migration of gases over considerable distances. They also point out the importance of faults and fractures in providing the means for the mass transport of gas. Therefore, it is assumed here that most of the rapid migration of CO_2 through soils at Kilauea Volcano is controlled by mass transportation processes rather than by diffusion. Gas mobility within the soil is probably controlled primarily by soil permeability, atmospheric meteorological factors (Reimer, 1987) and by faults and fractures.

Degassing of Kilauea

Kilauea's summit magma chamber, which is thought to be a dike and sill complex (Swanson et al., 1976; Ryan et al., 1981), extends from about 6 to 2 km depth under Kilauea caldera and sits above the primary feeder conduit (Ryan et al., 1981). Mantle sources supply magma to the summit magma chamber (Ellsworth and Koyanagi, 1977; Wright, 1984). Both the East and Southwest Rift Zones extend from Kilauea caldera. Magma accumulates in the summit chamber and is then discharged down the rifts (Dzurisin et al., 1984). The accumulation and withdrawal of magma from the summit region causes summit inflation and deflation (Dvorak and Okamura, 1987). The East rift receives most of this magma and is the site of the recent and present on-going eruptive activity at a cinder cone vent called Pu'u O'o (Heliker and

Wright, 1991 and Mattox et al., 1993). The Southwest rift has a poorly defined plumbing system (Dzurisin et al., 1984).

Degassing models for Kilauea have been presented by Gerlach and Graeber (1985) and Greenland et al. (1985). Gerlach and Graeber (1985) calculated the volatile budget of parental magma intruded into the summit reservoir. They used sulfur analyses in East-rift submarine basalts and glass inclusions to infer the weight percent of sulfur in the subsurface magma and then subtracted the sulfur in glassy Kilauean fountain spatter, in order to calculate the quantity of degassed sulfur. They then used the quantity of degassed sulfur, volcanic gas analysis and residual H_2O and CO_2 to calculate the weight percent of each volatile in the subsurface magma. Greenland et al. (1985) used: 1.) analysis of eruptive gases, 2.) geologic data on magma supply rates and erupted lava volumes, 3.) ground based COSPEC measurements of SO_2 emissions made in Kilauea caldera, and 4.) airborne infrared spectrometer measurements of CO_2 and SO_2 from summit fumaroles and the East Rift Zone in order to estimate the amount of volcanic emissions produced by Kilauea and the original content of gases in parental magma intruded into the summit reservoir. Both of these models are presented below and were used to infer the volatile content and degassing systematics of magma from Kilauea.

It has been recognized (Gerlach and Graeber, 1985) that Kilauea degasses in two main ways: 1.) one stage degassing and 2.) two stage degassing. Rarely, parental basaltic magma is injected directly into Halemaumau crater at the summit of Kilauea. The gases emitted from the basalt are referred to as Type 1 volcanic gas

(Figure 1A) and are characterized by higher CO_2 volume percents than Type 2 volcanic gas (Gerlach and Graeber, 1985). Normally, the parental basaltic magma is injected into the summit magma chamber where it resides long enough to fractionate. Later the magma is discharged down the East Rift Zone. Gas exsolved while the magma vesiculates in the summit chamber are termed chamber gases and these are emitted at the summit of Kilauea. The magma which migrates down the east rift emits Type 2 volcanic gas (Figure 1B) at the active east rift vents. Type 2 gas is characterized by much lower CO_2 concentrations (Gerlach and Graeber, 1985) than Type 1 gas, but the chamber gas has the highest CO_2 concentrations. The composition of chamber gas at 2 km depth is about 88 vol% CO_2 and 12 vol% sulfur. So, either the parental magma intruded into the summit reservoir erupts directly in a sustained summit eruption with Type 1 gas or it remains in the summit chamber, degasses most of its CO_2, and becomes degassed, reservoir equilibrated magma (Greenland et al., 1985; Gerlach and Graeber, 1985). Carbon dioxide measurements in this study were taken when the summit area was releasing chamber gas described by these models.

Using magma supply rates to the summit chamber between July, 1956 and April, 1983 and the weight percent of parental, stored and residual volatiles, Gerlach and Graeber (1985) were able to calculate the amount of H_2O, CO_2 and S entering Kilauea's summit chamber. Degassing occurred primarily by chamber gas and Type 2 volcanic gases through this time. Two-stage degassing has been the predominant means of gas escape from a Kilauean magma since 1924. When the parental magma

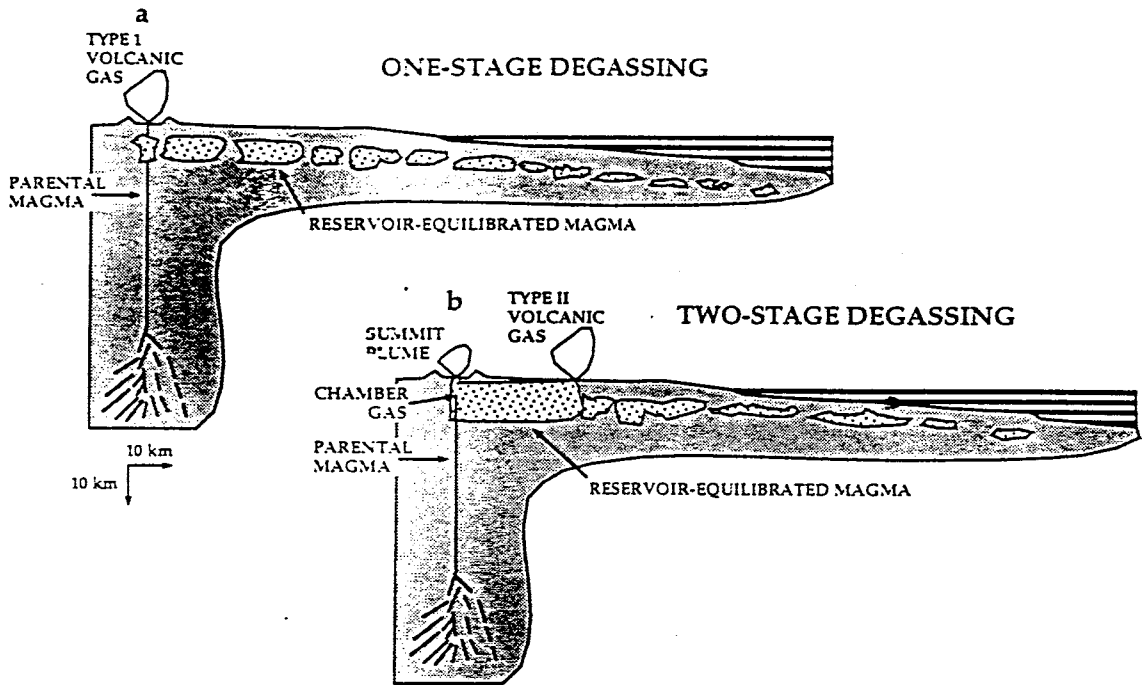

Figure 1. Gerlach's (1986) model for degassing at Kilauea volcano. Schematic cross sections, without vertical exaggeration, of the magma supply, storage and transport system. Each cross section starts west of Kilauea caldera and runs through Halemaumau crater, southeast along the upper east rift zone (ERZ), and east and northeast along the middle and lower ERZ. The cross sections continue along the submarine ERZ. The parental magma conduit is greatly exaggerated and the summit chamber is enlarged. (a) one-stage degassing permits Type I volcanic gas to be emitted during a summit eruption. (b) two-stage degassing involves venting of chamber gas from parental magma at the summit while a ERZ eruption emits Type II volcanic gas from reservoir-equilibrated magma (Gerlach, 1986). Diagram after Gerlach (1986).

degasses to reservoir-equilibrated magma, chamber gas venting emits most of the parental CO_2 at the summit (Table 1). Therefore, the summit of Kilauea releases large amounts of parental CO_2 and lesser amounts of H_2O and sulfur (Table 1). Chamber gas CO_2 discharged about 1000 to 5000 Mg CO_2/day (Gerlach and Graeber, 1985). The venting of chamber gas CO_2 accounts for about 94% of the CO_2 contained within the parental magma (Table 1).

Greenland et al. (1985) imply that summit degassing is largely limited to CO_2 and that magma intruded in the summit reservoir contains a very CO_2-rich fluid phase. They estimate, using the 1983 magma supply rate and summit fumarole emission rates, that 0.29 weight percent CO_2 and 0.029 weight percent SO_2 is lost at the summit by degassing of the summit reservoir (Table 1). They also estimate that 91% of the initial CO_2 content in the parental magma is lost in summit degassing.

Gerlach (1986) modeled the exsolution of H_2O, CO_2 and S as magma rises from a shallow crustal reservoir underneath Kilauea volcano. This model predicts that volatiles do not vigorously exsolve from an ascending magma until it reaches shallow depths ($\leq$ 150 m lithostatic, $<$ 3 MPa). Most S and H_2O is exsolved below 2-3 MPa ($<$ 100-150 m lithostatic) while much of the CO_2 contained in the magma is exsolved at greater depths (about 1 km, 10 MPa). This implies that as magma rises underneath Kilauea volcano, CO_2 is the first species exsolved into a vapor phase (Gerlach, 1986). This is important to this study in that CO_2 is the first gas exsolved from Kilauea magma, so it is probable that it will be the first gas to be vented into the atmosphere as magma rises. Also, CO_2 that degasses from magma at depth provides a source for

Table 1. Calculations of parental magma concentrations and percent CO_2 lost from the parental magma due to summit degassing from (1) Gerlach and Graeber (1985) and (2) Greenland et al. (1985).

Weight % concentration of parental magma when it arrives at the summit reservoir		
	(1)	(2)
H_2O	0.30	0.32
CO_2	0.65	0.32
S	0.13	0.09

Percent of initial magmatic CO_2 lost to summit degassing		
	(1)	(2)
H_2O	10%	9%
CO_2	94%	91%
S	46%	18%(SO_2)

CO_2 emitted through soils in the area. In general, all these models and calculations (Gerlach and Graeber, 1985; Greenland et al., 1985 and Gerlach, 1986) predict significant summit venting of CO_2 with very small amounts of H_2O and sulfur.

Study Area

The study area is located at Kilauea Volcano, Hawaii (Figure 2). All samples were taken within Kilauea caldera (mainly around Halemaumau crater) and across the Southwest Rift Zone (SRZ). Soil gas samples were collected and measured for CO_2 within Kilauea caldera (Area 1, 2 and 3) and along nine transects across the SRZ (Figure 2). Kilauea caldera formed by subsidence, or massive withdrawal of magma from a reservoir beneath the summit (Moore and Trusdell, 1993) and is bounded by a series of ring faults (Cox, 1983). There are many recent lava flows within the caldera and along the SRZ. The entire study area is underlain by pahoehoe and aa basalt flows of various ages (Peterson, 1967). The Puna Basalt Formation covers most of the surface of Kilauea (Holcomb, 1987). Holcomb (1987) recognized that the Puna Basalt covering about 90% of the surface is less than 1100 years old and 70% is less than 500 years old. The Keanakakoi Ash Member is part of the Puna Basalt Formation and consists of phreatomagmatic and phreatic fall and surge deposits (McPhie et al., 1990). Some exposures of the ash member to the south and southwest of Kilauea caldera are 5 to 12 meters thick and, for the most part, decrease in thickness to the southwest of the caldera (McPhie et al., 1990).

Several cracks and fractures exist in the lava flows within the caldera and

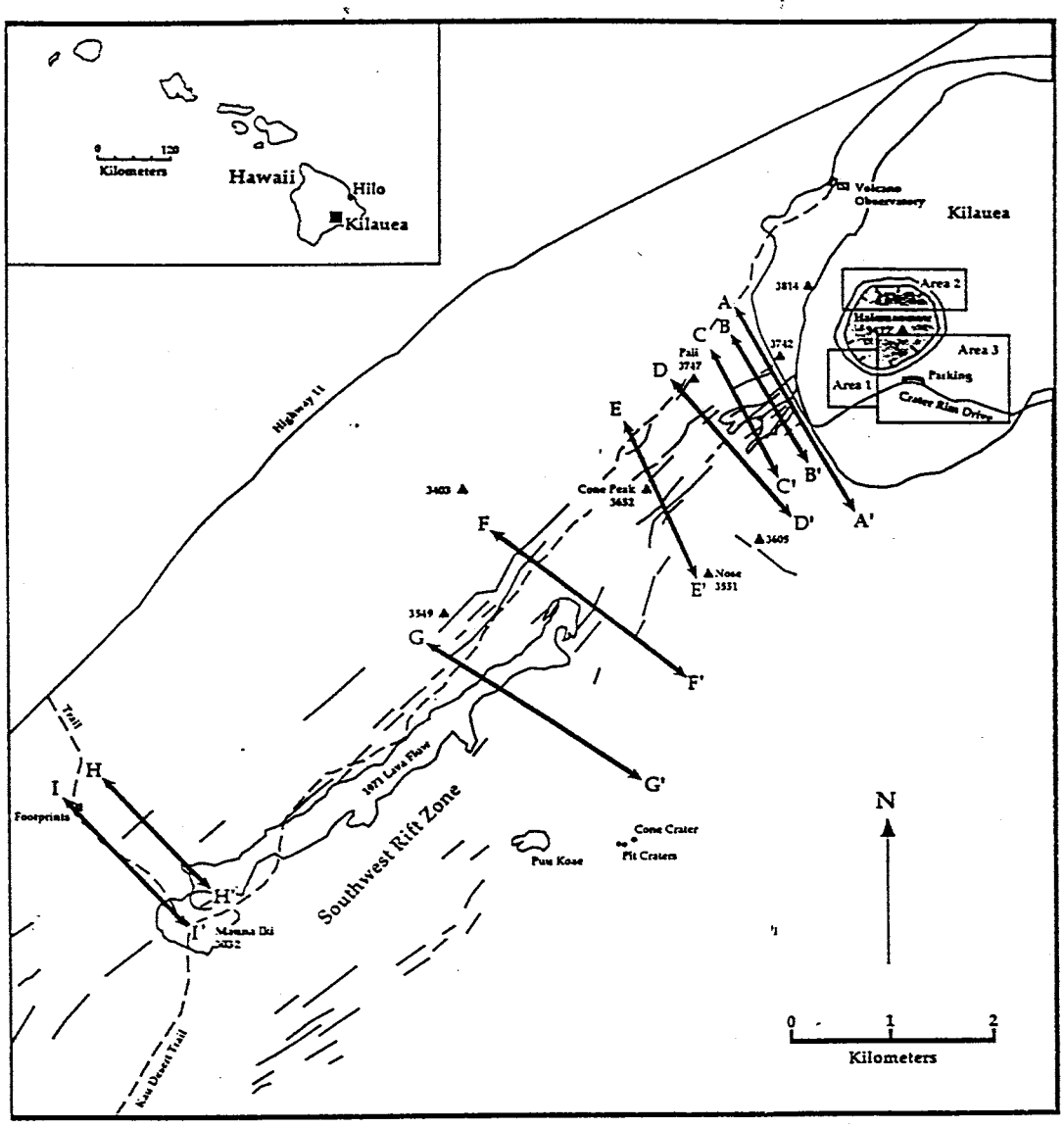

Figure 2. The study area is located upon Kilauea volcano. Two main study areas include: 1.) three areas (Area 1, 2 and 3) around Halemaumau and 2.) nine transects (A through I) across the Southwest Rift Zone. Triangles represent benchmarks and the dark solid unlabeled lines represent cracks. Inset: The location of Kilauea upon Hawaii.

along the SRZ. These cracks vary from a few centimeters to 5 meters wide (Peterson, 1967). These fracture systems provide passage ways for the emission of gas and steam (Cox, 1983; Reimer, 1987). Several small steam and gas plumes are visible throughout these areas but most prominently within Kilauea caldera. Within the study area, around Halemaumau crater, there are many of these features. Many of these thermal areas have been described by Casadevall and Hazlett (1983) although many have not. The northern half of Area 1 (Figure 2) contains large areas of soil which show visible steam and gas plumes. Soils in this area exhibit either mineral precipitation within the soil or soil alteration. Visually observation suggests that this area is the most active steaming area in this study. Many steam and gas vents also occur throughout Areas 2 and 3. The most prominent area of steam and gas venting besides Area 1, is the far western corner of Area 3 which is located next to a fissure or crack.

Due to the northeast trade winds, windward and leeward climatic conditions at the summit vary greatly. Windward, to the north and east of Kilauea caldera, soils promote the growth of tropical vegetation. Areas to the south and west of the caldera have limited soil development and support little to no vegetation. Many of the lava flows are overlain by soils which have been surveyed by the United States Department of Agriculture (USDA) in 1973. All of the measured sites on the SRZ are in extremely gravelly sand, about 20 cm thick, underlain by stratified layers of volcanic sand, gravel, cinders and pumice (USDA, 1973). A representative soil profile of the SRZ portion of the study area is shown in Figure 3. The depth to bedrock varies

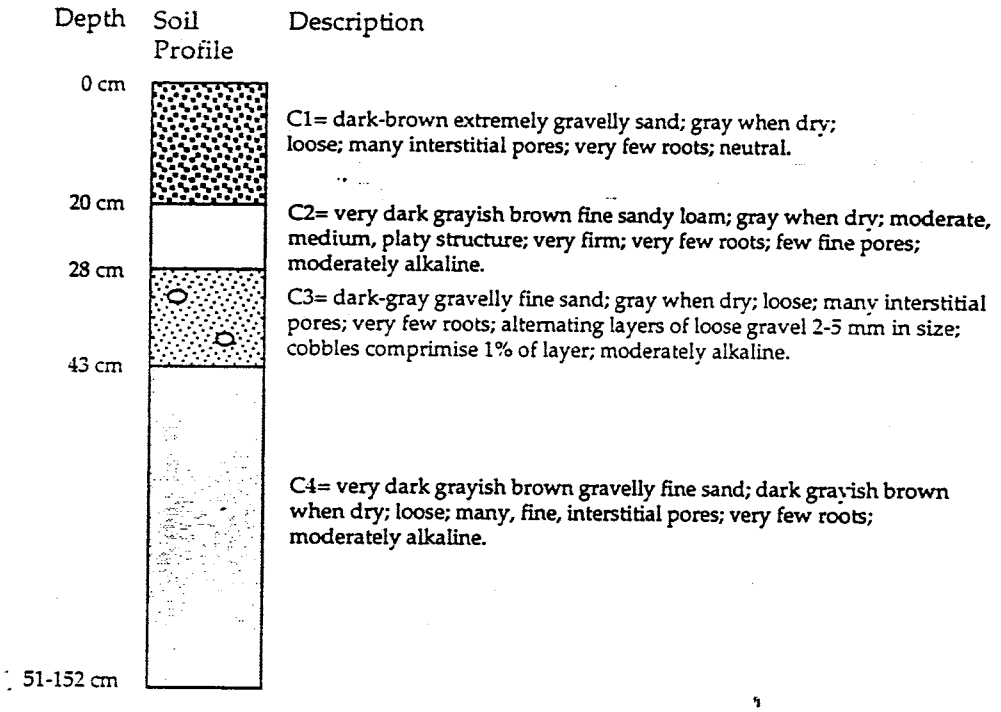

Figure 3. A representative soil profile, adapted from USDA (1973), in most parts of the study area. Soil depths range from 51 to 152 cm. This profile was taken at: lat. 19°24'12" N. and long. 155°31'40" within the Kilauea Crater Quadrangle (USDA, 1973).

from 50 to 150 cm and there are shallow sandy soils (less than about 50 cm thick) in some areas (USDA, 1973). Permeability is "rapid" and runoff is "slow", according to the USDA (1973).

Area 1, 2 and 3 soils, in Kilauea caldera and around Halemaumau crater (Figure 2), consist mostly of this same extremely gravelly sand but have patches of a coarse (>1 cm) basaltic tephra on the surface. This material commonly mantles some of the basalt flows and is extremely porous and thin. These areas also have basalt flows outcropping at the surface. The soil within the study area around Halemaumau is generally thin (0-55 cm) or non-existent in some places. We attempted measurements in some areas across the East Rift Zone but, because of heavy vegetation and the limited existence of soil (recent basalt flows), it was found difficult.

Methods

Two methods were used to measure soil CO_2 flux from Kilauea Volcano. First, soil gas CO_2 concentrations (SGCC) were measured at depth using a CO_2 probe throughout the study area in order to determine where the greatest amounts of CO_2 occurred. If CO_2 concentrations were relatively high (>400-500 ppm), soil gas CO_2 flux (SGCF) measurements were made on top of the soil to determine CO_2 emission rates at each site. Both CO_2 probe (SGCC) and flux measurements (SGCF) were taken in the areas described above. All measurements were taken between July 26, 1993 and August 27, 1993. Carrying out measurements by the methods described

below is difficult in these areas due to the limited amount of soil, the absence of soil and, in places, a cemented thin crust has developed on the surface. Therefore, measurements were carried out wherever possible along the SRZ transects and around Halemaumau.

All SGCC and SGCF measurements were made in the field using a LICOR LI-6262 Analyzer. The LI-6262 is a differential, non-dispersive, infrared gas analyzer which uses reference and sample cells to calculate the concentration of CO_2 in a gas sample. The LI-6262 was run in absolute mode which analyzes CO_2 alone. Measurements were made in the low resolution mode (0-3000 ppm CO_2) with an accuracy of ± 2 ppm at 1000 ppm and $< \pm 6$ at 3000 ppm total concentrations. The CO_2 analyzer's span and zero were calibrated every day before measurements were taken using a soda lime/CO_2 absorbent for the zero calibration and a calibration gas (2,000 ppm CO_2) for the span. The reproducibility of the standard gas was $\pm$ 2%.

The probe used for SGCC was described in McCarthy and Reimer (1986) and in Reimer (1990) and are slightly modified. Probe measurements of CO_2 were taken by inserting a hollow (inside diameter is about 1.5 mm) stainless steel rod 10 to 85 cm into the ground. A thin steel wire was placed within the hollow rod, before inserting the rod into the ground, to avoid blocking of the gas collection holes. This wire was removed after the probe was in place. Measurements were made at various depths when possible. The soil gas was pumped from the soil through the steel rod and into the LICOR (LI-6262) infrared spectrometer (Figure 4A).

Flux measurements were made by the accumulator flux chamber method

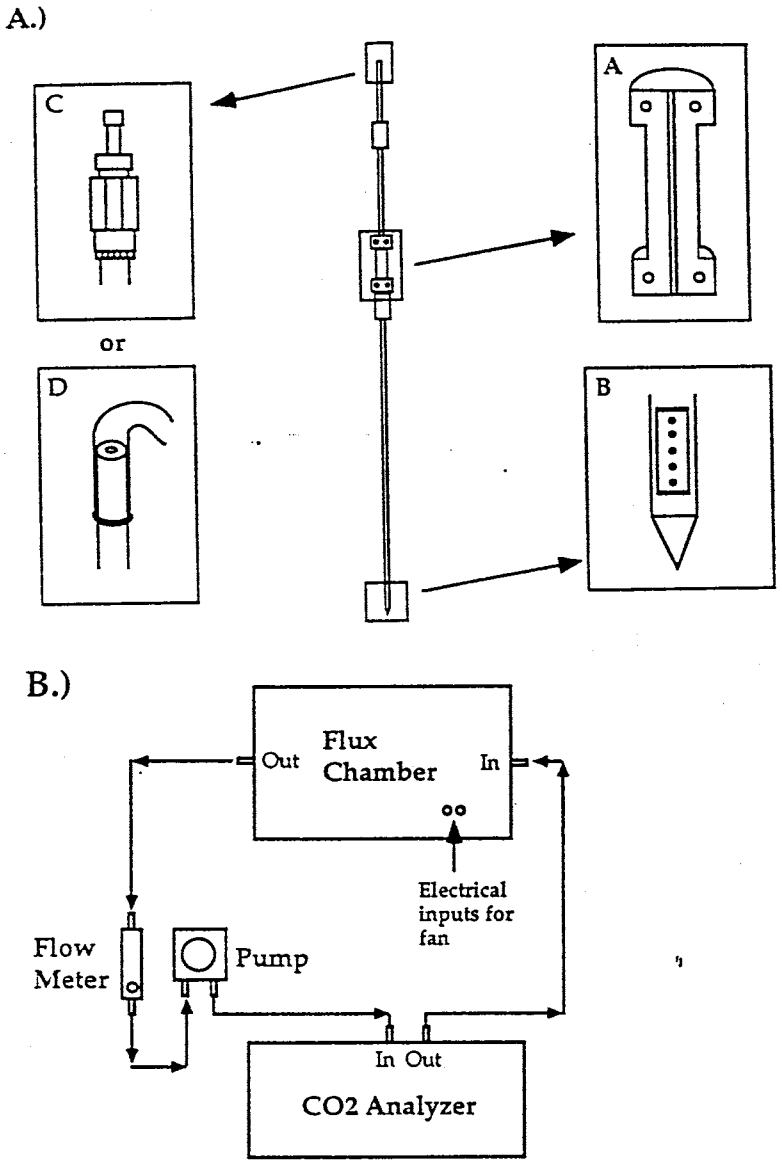

Figure 4. A.) Schematic drawing showing soil probe used to take SGCC and soil gas samples for carbon isotopic analysis. A tube was fit on the top of the soil probe when CO_2 concentrations were being measured with the CO_2 analyzer. A special septum was attached to the top of the soil probe to collect gas samples. The probe was equipped with a threaded bottom so the probe could be cleaned and a slide hammer. B.) Schematic diagram showing the setup for measuring soil gas CO_2 fluxes. As gas builds up in the accumulator, a fan mixes the gas and it is pumped away through a flow meter and into the CO_2 analyzer. Gas analyzed returns to the accumulator. The pump, fan and analyzer were connected to a battery.

described by Kanemasu et al. (1974), Schery (1989) and Wilkening (1990) (Figure 4B). An aluminum box (33x22x15 cm) was placed open end 1 to 2 cm in the soil. A small electric fan was mounted inside the accumulator to mix the gas. Gas collected in the box was pumped out continuously and fed through a flow meter, and analyzed in the LICOR CO_2 Analyzer (Figure 4B), before being returned to the accumulator. Measurements of CO_2 were taken every 10 seconds for approximately 250 seconds, depending on the concentration increase, to determine the rate of CO_2 buildup within the box. This time period was chosen because it provided a slope or flux over a very short period of time so that more field measurements could be made. Soil CO_2 emission rates were calculated by plotting the CO_2 concentrations over time and performing linear regressions in order to determine the slope of the line, this in turn gave the flux.

A standard site was chosen to determine the reproducibility of the flux chamber method over the study period. Later, this standard site consisted of two sampling locations (B and C) which are located near the edge of Halemaumau. These sites are about 1.5 meters apart. Each site was measured on various days when possible.

Soil gas samples were also taken by pumping gas from the ground through a soil probe and into evacuated Tedlar gas sampling bags. These samples were analyzed for carbon isotopic ratios. Small volumes of the gas sample were pumped from the sample bags using a hypodermic needle and septum, and introduced into an evacuated line small aliquots at a time. A ethylene glycol trap froze out any existing water and a liquid nitrogen trap froze out all CO_2 within the sample. The

noncondensible gas was then pumped out and the CO_2 transferred to a sample bottle. Isotopic measurements were made on a Finnegan MAT delta-E mass spectrometer at New Mexico Institute of Mining and Technology (NMIMT). All samples were analyzed relative to PDB and are expressed as $\delta^{13}C$ (per mil) with an error of $\pm$ 0.1 per mil.

Soil samples were collected from 10 to 25 cm depth at five localities and later analyzed for their microbial CO_2 production. The methods are described in Stotzky (1965). Samples were weighed and placed in sealed glass bottles with septums. These bottles were kept incubated at 22°C over time to allow the microorganisms to produce CO_2. This gas was removed with a hypodermic needle and introduced into a gas chromatograph to analyze the concentration of CO_2 production through time.

Results

Standard Measurements

Measurements of CO_2 in the accumulator, taken over time, were plotted to obtain emission rates of CO_2. During 07\28\93 to 08\02\93, SGCF measurements were taken in the same general area in order to determine the reproducibility of these measurements. At first, a site was chosen with an area of about 2.3 m^2, in order to perform these measurements. It was thought at first that such a small area would not have a large variation of SGCF so that measurements could be made anywhere within the area. Figure 5A shows the measurements taken within this area. The calculated fluxes are shown to the right of the dates and range from 7 to 64 $x10^{-3}$ $kg/m^2/year$

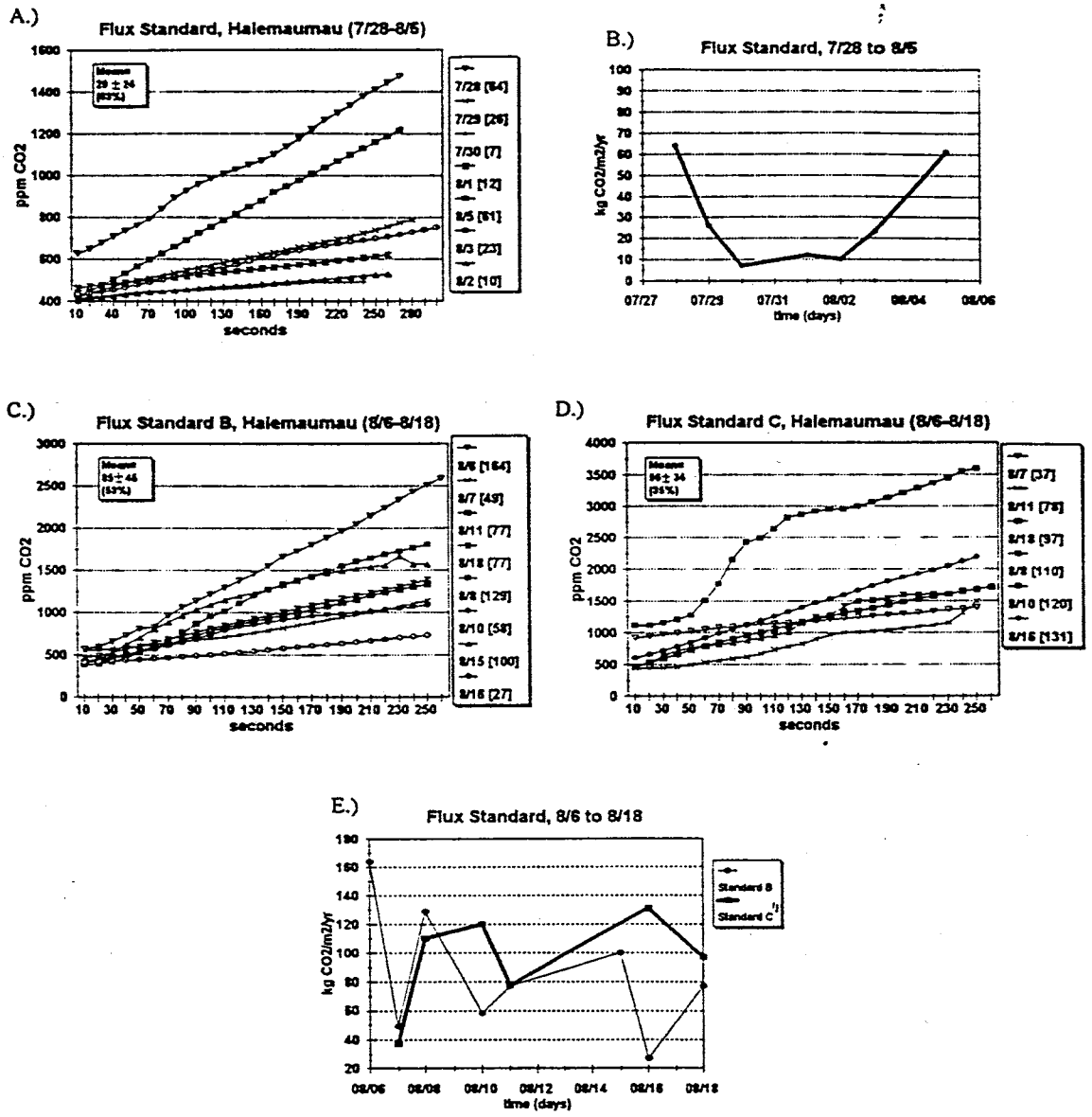

Figure 5. A) Graph shows CO_2 concentration through the time of sampling at the standard site. Measurements were taken from 07/28/93 to 08/05/93. The legend indicates the date and, in parenthesis, the CO_2 flux in $kg/m^2/yr$. B) Graph shows the flux of CO_2 through the time of sampling at the standard site. C-D) Graphs show CO_2 concentrations through time of sampling at standard sites B and C. Measurements at these sites were taken between 08/06/93 and 08/18/93. As above, the legend indicates the date of each measurement and the calculated CO_2 flux (same units as above). E) Graph shows the CO_2 flux through the time of sampling at standard B and C. On graphs 5A, 5C and 5D, the mean is shown and the coefficient of variation is in parenthesis.

with a mean of 29±24 kg/m^2/yr (coefficient of error= 83%) (Figure 5A). One spurious measurement of 398 kg/m^2/yr was ignored because it does not fall within the third standard deviation of the data set and is probably a product of variation due to some meteorological factor. Each SGCF measurement produced a linear relationship with time but the slopes vary from day to day and from place to place indicating varying CO_2. emission rates. Figure 5B displays the variation of flux over time within this general area.

As some variability was observed in the measurements within this 2.3 m^2 area, two sites (B and C) were chosen and the SGCF was monitored at the same site between 08\06\93 to 08\18\93. The results are shown in Figures 5C, 5D and 5E. Once again, each measurement of CO_2 in the accumulator produced a linear relationship with time at each site. The slopes of each line (or flux) changed over time. Site B ranges from 27 to 164 and, Site C from 37 to 131 kg/m^2/yr. Site C also had one spurious measurement of 360 kg/m^2/yr which was ignored because it is falls outside the third standard deviation range and is probably representative of variability caused by meteorological factors. Figure 5E displays the SGCF through the study period at each site.

Variation from day to day at each of the standard sites may be a function of the sampling method. To deduce the precision, standard deviations (1 σ) were calculated for site B and C (Figure 5 C-D). The standard deviation ranges from ± 35% (standard C) to ± 53% (standard B). The percent error of all CO_2 flux measurements range between ± 35% (standard C) and ± 53% (standard B).

Microbial Activity

Five representative soil samples were examined for their microbiologic CO_2 production to investigate the magnitude of their CO_2 contribution to the soil gas. Table 2 lists these values. These values all have the same magnitude (10^{-5}) with a mean of about 2.92×10^{-10} mg CO_2/gram dry weight (gdw)/hour (or 2.56×10^{-7} kg CO_2/gdw/year). Due to this minimal mean CO_2 production and the fact that most of the study area is devoid of vegetation, the organic CO_2 contribution is considered to be negligible compared to the concentrations and fluxes obtained here. However, analysis of microbial CO_2 production was determined under room temperatures while heating of the soil during daytime could possibly increase the amount of microbial CO_2 production. Therefore, the values in Table 2 are minimum estimates.

Carbon Isotope Measurements

Eight gas samples were collected in and around Kilauea caldera and analyzed for their isotopic composition ($\delta^{13}C$ in per mil). Figure 6 exhibits both the sample localities and $\delta^{13}C$ per mil. Sample 7 (-21.2 per mil) was taken within a fern forest in order to compare organic $\delta^{13}C$ with magmatic $\delta^{13}C$ in the area. Sample 8 (-2.7 per mil) was collected in the soil next to steaming vents to observe any variations between carbon isotopic ratios within the study area and around the study area. Samples 1-6 are all within the study area and have a $\delta^{13}C$ range of -1.9 to -7.4 per mil with a mean of -3.8 per mil. SGCF and SGCC were measured at each of these sites and are listed in Table 3. A direct correlation can be seen between $\delta^{13}C$ and SGCF as displayed by Figure 7. Higher $\delta^{13}C$ measurements ($>$-5.0 per mil) seem to correlate with higher

Table 2. Soil CO_2 emission rates from microbial activity for various soils within the study area.

Soil #	CO_2 produced ($mgCO_2$/gram dry weight/hour)
Soil 1	3.22×10^{-5}
Soil 2	2.48×10^{-5}
Soil 3	3.25×10^{-5}
Soil 4	2.30×10^{-5}
Soil 5	3.33×10^{-5}
mean	2.92×10^{-5} (or 2.56×10^{-10} $MgCO_2$/gdw/yr)

Table 3. $\delta^{13}C$, CO_2 flux and probe concentrations at gas samples collected for isotopic study. CO_2 fluxes are $kg/m^2/yr$ and CO_2 concentrations are in ppm.

Site #	$\delta^{13}C$ (o/oo)	CO_2 flux	CO_2 concentrations (depth=cm)
1	-2.4	100	>3000 (10)
2	-1.9	4198	>3000 (10)
3	-2.9	182	>3000 (50)
4	-2.9	38	>3000 (50)
5	-7.4	1	>3000 (50)
6	-5.1	8	>3000 (10)

Table 4. Ranges and the mean CO_2 concentrations (in ppm) measured with a probe along transects A through I.

Transect	range of CO_2	CO_2 mean
A	384- >3000	706
B	424- >3000	1716
C	259- >3000	1566
D	169- >3000	957
E	103-509	356
F	258-539	379
G	215-420	326
H	200- >3000	880
I	388-2364	1044

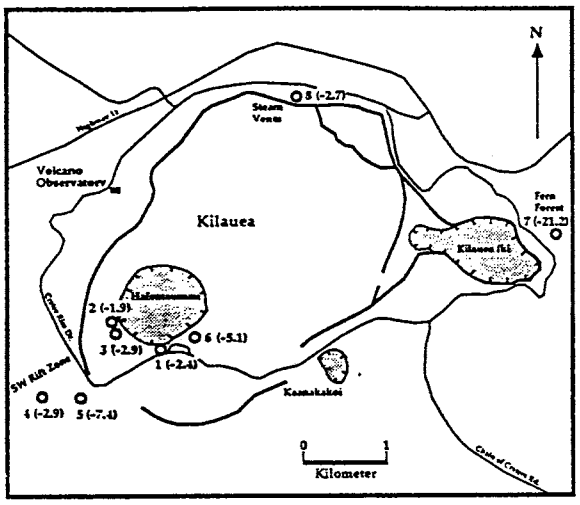

Figure 6. Map displaying gas sampling sites for $\delta^{13}C$ analysis. $\delta^{13}C$ values are located next to the sample site number in parenthesis. All $\delta^{13}C$ values are relative to PDB and the units are per mil. The carbon isotopic values are listed in Table 2.

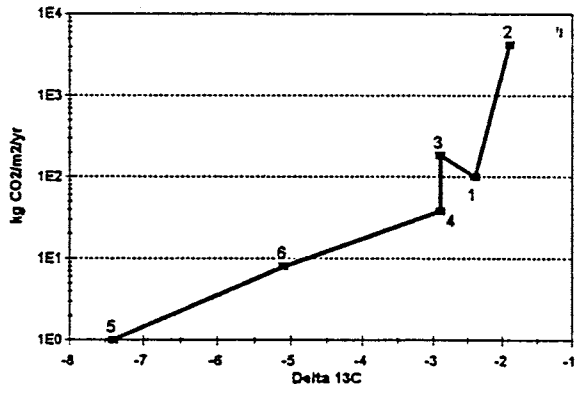

Figure 7. Graph showing $\delta^{13}C$ (in o/oo) versus CO_2 flux. Data for this graph is listed in Table 2. Other studies indicate that magmatic derived CO_2 at Halemaumau range from -2.54 to -4.16 per mil (Gerlach and Thomas, 1986) and about -2.0 to -3.9 per mil (Friedman et al., 1987).

fluxes (>10 kg $CO_2/m^2/yr$). Friedman et al. (1987) report that $\delta^{13}C$ values for volcanic gas at Halemaumau are around -3.5 $\pm$0.3 per mil ranging from -1.9 to -3.9 per mil. Gerlach and Thomas (1986) report a $\delta^{13}C$ range of -2.54 to -4.16 per mil with a mean of -3.14 per mil for Kilauea summit fumaroles. Rubin et al. (1987) report $\delta^{13}C$ values ranging from -3.0 to -3.6 per mil for juvenile magmatic gas in the fumaroles at the summit of Kilauea. Samples 1 through 4 fit into these ranges whereas samples 5 and 6 have lower values.

Soil Gas CO_2 Concentrations

SGCC's were measured to find CO_2 gas anomalies so that CO_2 flux measurements could be made. Probe sample locations for Area 1 and 2 are located on Figure 8A. Carbon dioxide concentrations (in ppm) are plotted on Figures 8B and 8C. Probe measurement sites on the SRZ are located on Figures 9A, 9B and 9C. All measurements were taken at depths ranging from 5 to 85 cm (Appendix A). These depths were dependent on the soil thickness. In all cases the sampling probe was inserted as far as possible up to a maximum depth of 85 cm. Figure 8B (area P1) and 5C (area P2) show the CO_2 concentrations (in ppm) encountered around Halemaumau crater. In area P1, values range from 400 to >3000 ppm with a mean of about 1835 ppm. Area P2 has SGCC's ranging from 502 to >3000 ppm with a mean of 1837 ppm. Both areas (P1 and P2) show concentrations well above atmospheric CO_2 concentrations (about 332 ppm) at depths ranging from 5 to 85 cm.

SGCCs were also measured along nine transects across the SRZ. Figures 10 and 11 display the SGCC (in ppm) at depth along each transect. Cracks which pass

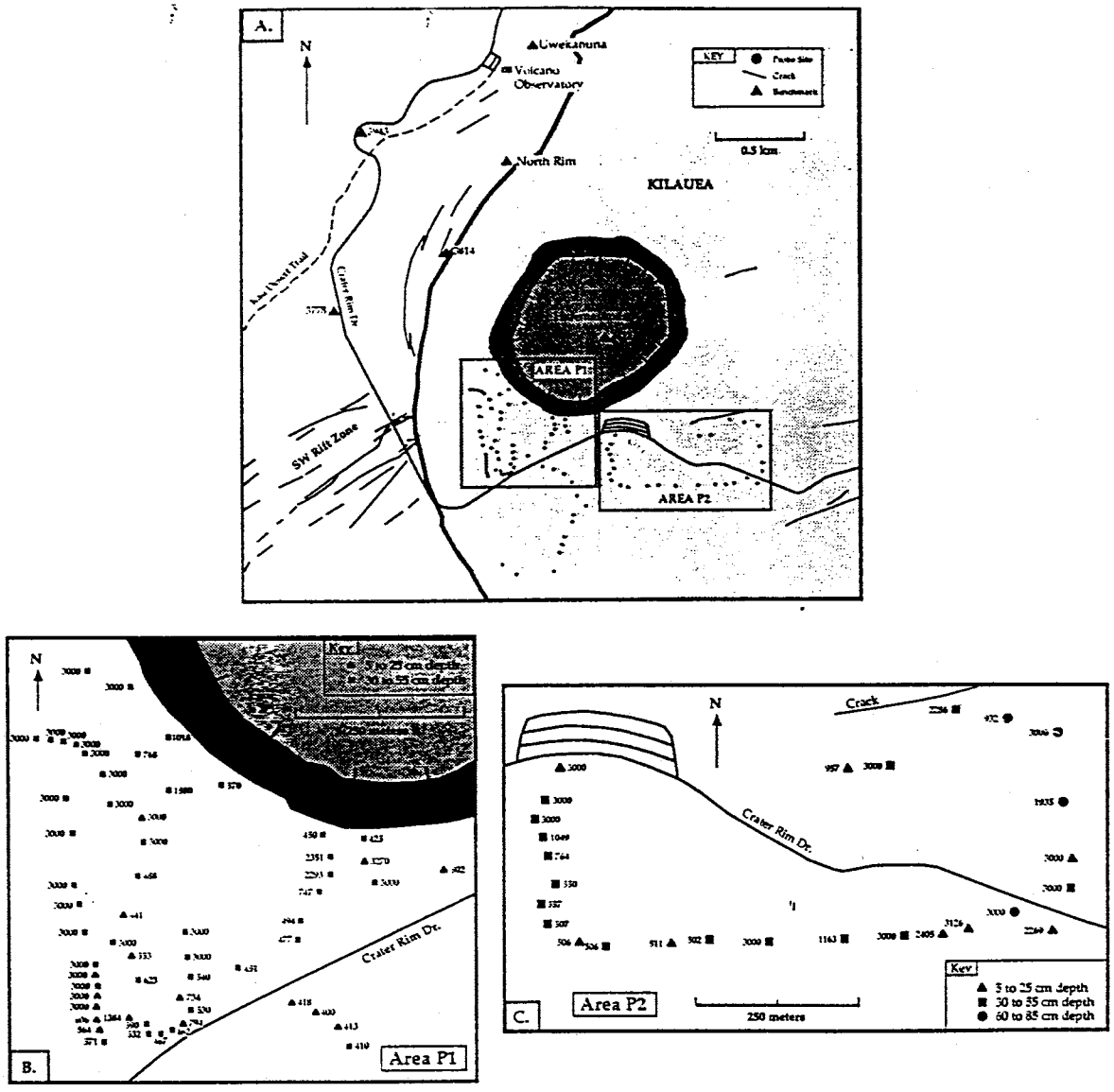

Figure 8. A.) Map showing CO_2 probe measurement sites around Halemaumau. B.) Map showing SGCC and depth within Area P1. C.) Map showing SGCC and depth within Area P2. All measurements are in ppm and all points labelled 3000 are minimums.

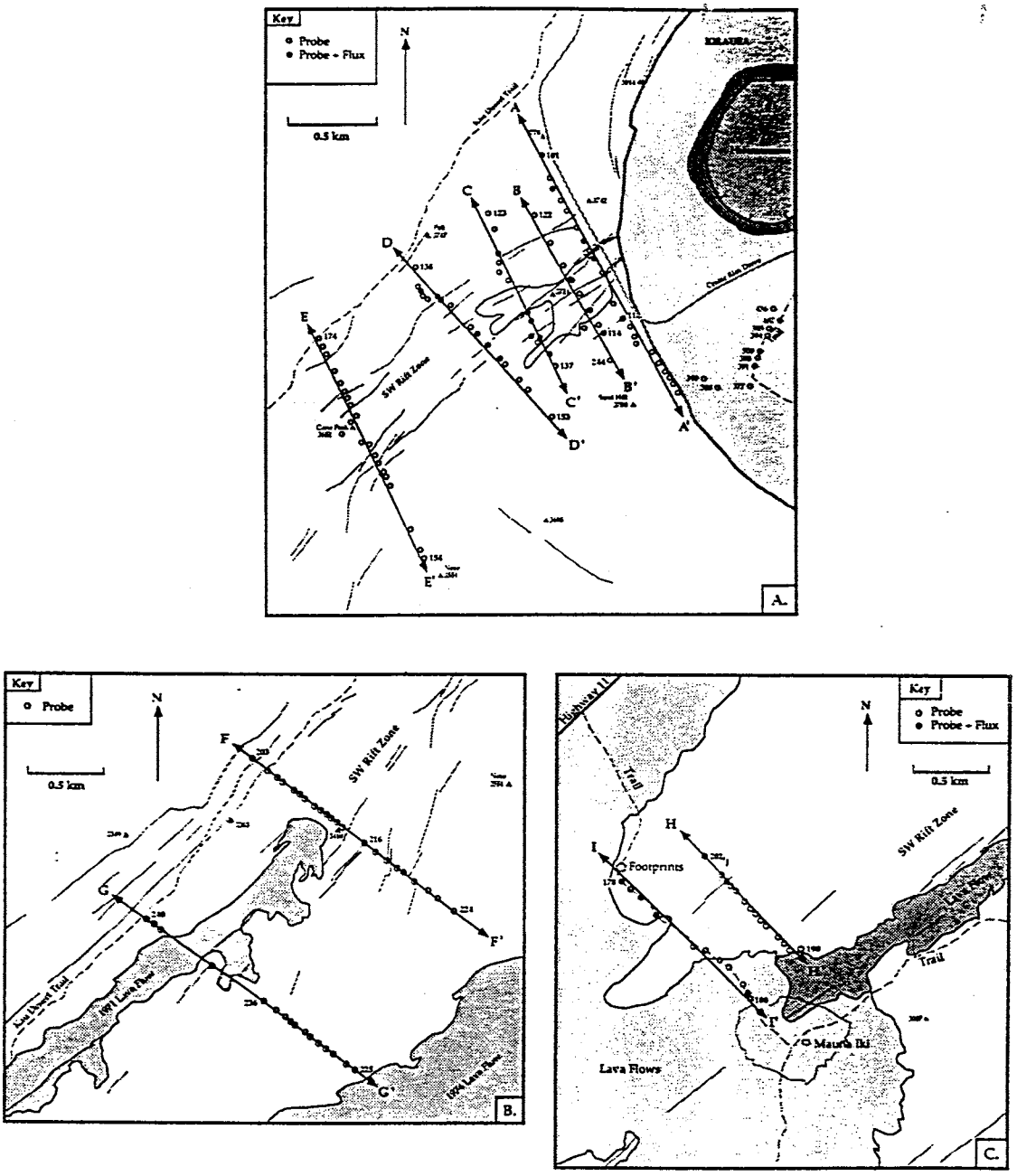

Figure 9. Map showing locations for both SGCF and SGCC measurements along transects: A.) A to E, B.) F and G and C.) H and I. Numbers within caldera (in 9A) are probe CO_2 concentrations in ppm. Numbers along transects are sample location numbers for reference.

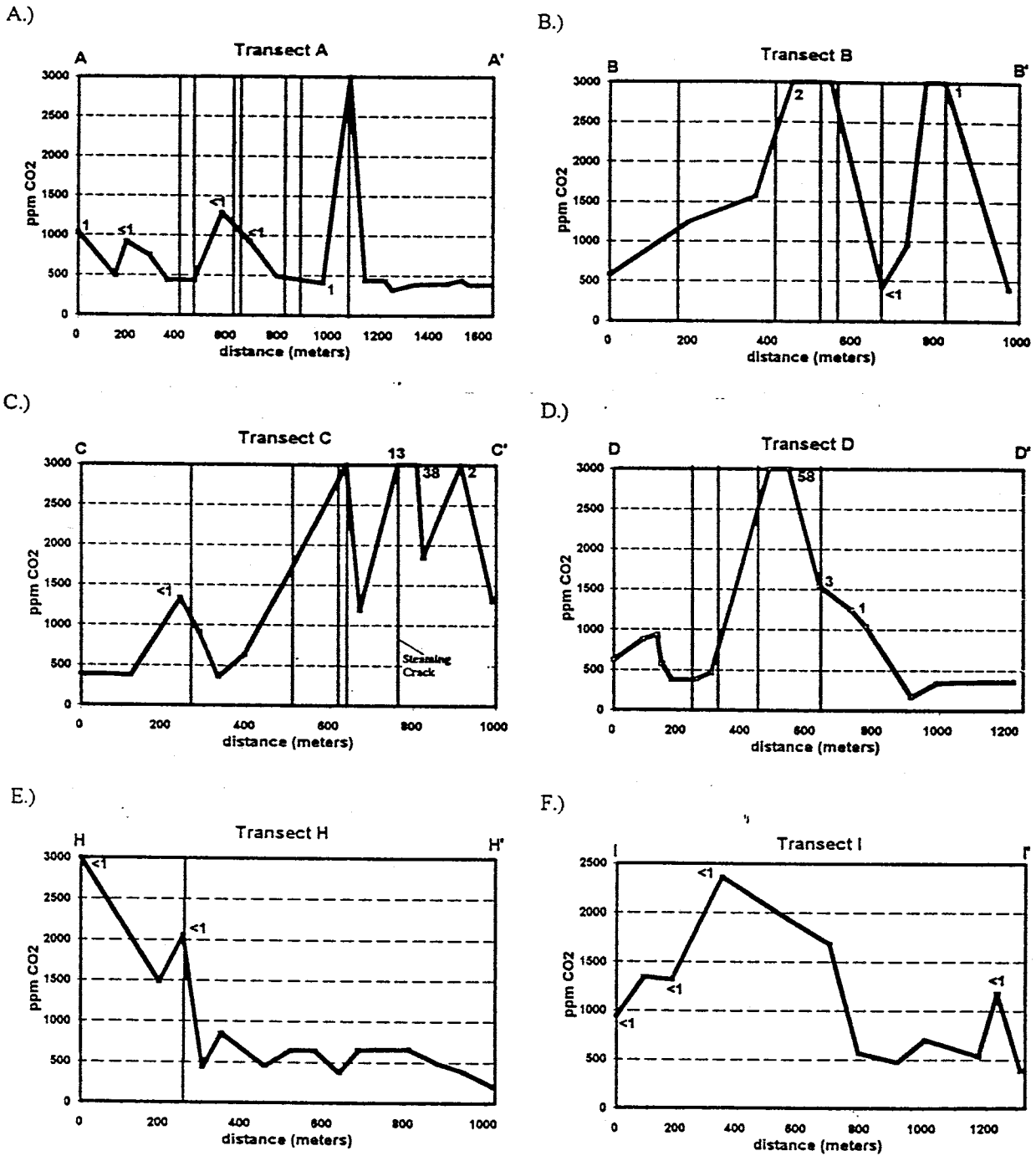

Figure 10. A-F) Figures showing CO_2 concentrations at depth along transects A-D, H and I measured with a probe. Carbon dioxide fluxes (in kg/m^2/yr) taken at a probe site are located on each figure. Vertical dark lines represent visible cracks on the surface.

A.)

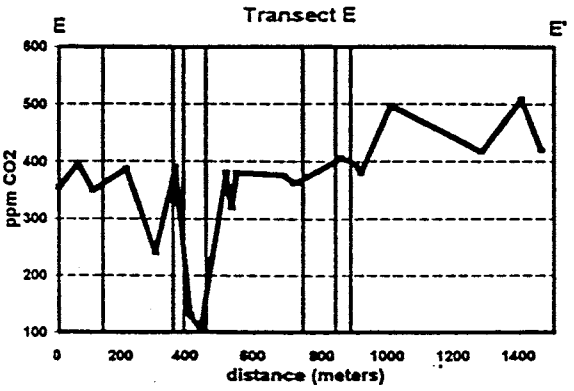

B.)

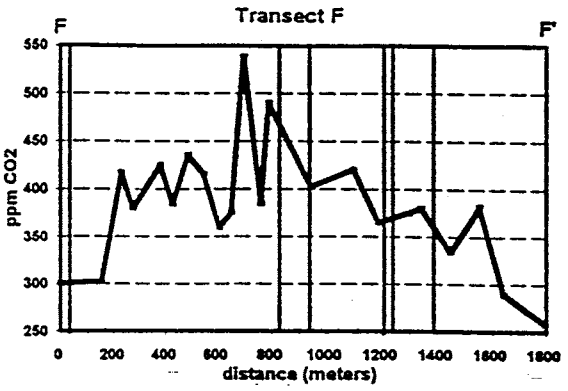

C.)

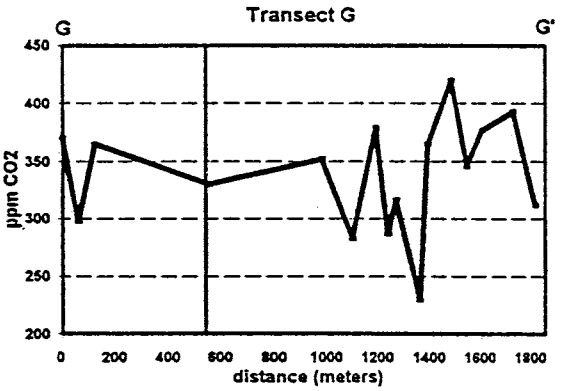

Figure 11. A-C) Figures showing CO_2 concentrations at depth along transects E-G measured with a probe. Dark vertical lines represent cracks. Fluxes along these transects were non-existent.

through a transect are located on each figure. Depth measurements at some sites along the SRZ showed an increase in CO_2 with depth. On the other hand, there seems to be no correlation between variations in the depth of measurement between sample sites and higher CO_2 concentrations. That is to say that even though CO_2 concentrations at each site along a transect were taken at different depths, there was no correlation between the highest CO_2 concentrations and lowest depths or vice-versa. On the other hand, the position of a sample site relative to cracks is noted because it might result in higher CO_2 concentrations due to the mass transport of CO_2 through cracks or weaknesses within the rock. Figures 10 and 11 show that SGCCs are not affected by these cracks because in many cases, high CO_2 concentrations occur far away from them. On the other hand, in some instances, such as Transect C (Figure 10C), cracks seem to control the SGCC. Along Transect C, steam was observed emanating from one of these cracks (indicated on Figure 10C). This is the only location within the SRZ study area that visible steam was observed emanating from a crack. This steaming fissure has been described by Casadevall and Hazlett (1983). The location of steam emitting cracks seems to sometimes control the SGCC. The $\delta^{13}C$ value at this site along transect D is -2.9 per mil which suggests a magmatic source for the gas emitted from this crack.

Ranges and mean SGCC for each transect are presented in Table 4. Some of the lower ranges drop below atmospheric (Table 4). This suggests a possible CO_2 sink at depth but it is unknown what factors are responsible for this. Transects A-D, H and I all have mean SGCCs greater than 700 ppm whereas mean SGCCs for

transects E-G are all under 400 ppm. Also, the range of SGCCs in transects A-D, H and I start below atmospheric values and extent to values greater than 2300 ppm.

Rates of Soil CO_2 Emission

Soil gas CO_2 emission rates were measured to evaluate the percent of CO_2 leaking from soil as opposed to fumaroles and active areas of degassing. Flux sample locations for areas 1, 2 and 3 are located on Figure 12A and in Appendix B. Carbon dioxide emission rates (in $kg/m^2/year$) are plotted on Figures 12B-12D. Flux measurement sites on the SRZ are located on Figures 9A-9C. As discussed in a previous section, the precision of all SGCF measurements presented in this study ranges from $\pm$ 35% to $\pm$ 53%. SGCFs were measured and plotted in order to determine the slope of the line which in turn gave the CO_2 flux (Appendix B). When linear regressions were performed on each line, to determine the slope, there were two basic types of trends shown in 86 sample sites. About 76% of the flux measurements were highly linear as demonstrated in Figure 13A and 13B. About 24% of the flux measurements had two different slopes associated with them (Figure 13C and 13D). Linear regressions were made through the first slope obtained and usually were characterized by a higher slope (Figure 13C and 13D). After a large increase, these points level off and gradually increase compared to the first set of points. The reason for this change in slope has not been studied but it is speculated that it might have something to do with a poor seal with the soil which allows gas to leak from the accumulator, gas diffusion back into the soil due to pressure or wind forcing the air from or into the accumulator. Due to these factors, the initial slope

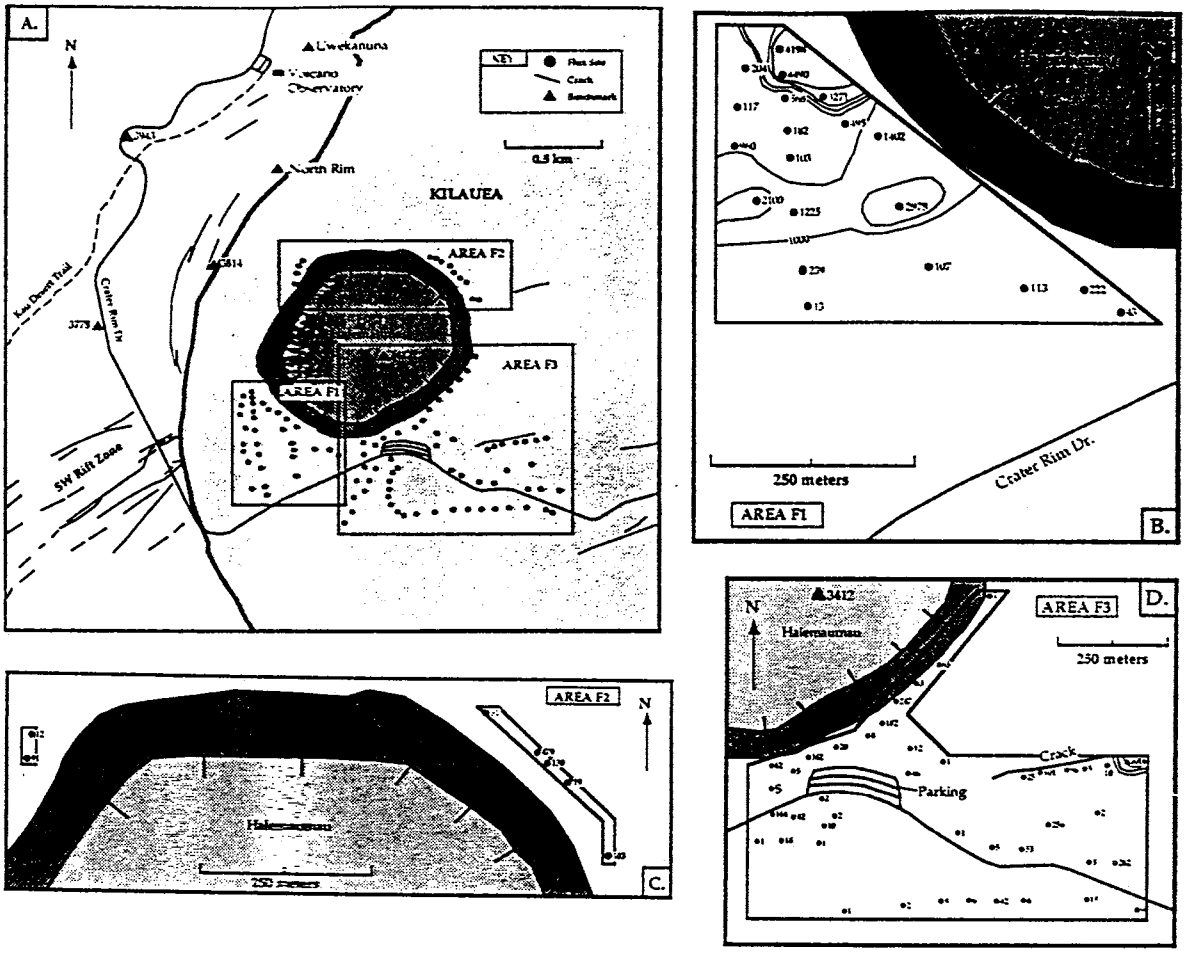

Figure 12. A.) Map showing CO_2 flux monitoring sites around Halemaumau (S= Standard Site). B.) Map showing SGCF (in $kg/m^2/yr$). C.) Map showing CO_2 emission rates from Area F2 (same units as above). D.) Map showing CO_2 emission rates for Area F3 (same units as above). Contour interval is 1000 $kg/m^2/yr$.

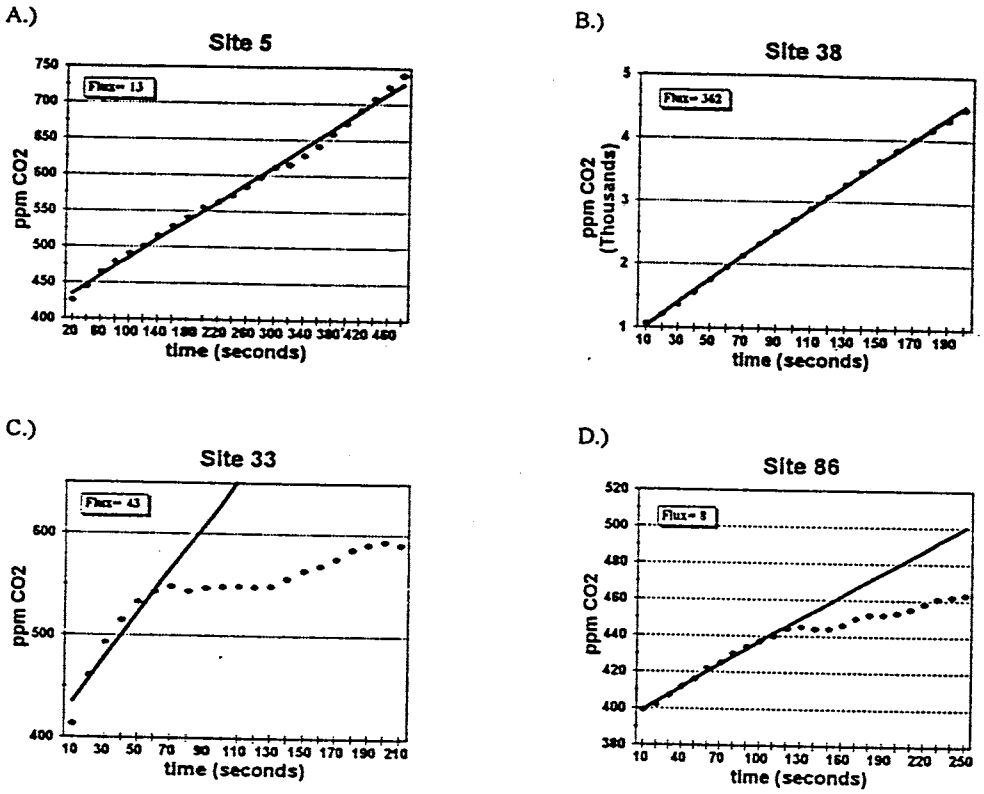

Figure 13. Figures displaying CO_2 concentration through time as measured by the accumulator method. Lines are linear regression lines from which slopes and soil CO_2 fluxes were calculated. A-B) These figures are examples of about 76% of the data presented here for CO_2 flux. C-D) These lines represent about 24% of the CO_2 flux data. Regression lines were taken over the first increase of CO_2 while the second linear array is thought to be a function of CO_2 leaking from the flux chamber.

is thought to be more representative of the CO_2 flux (pers. comm. G.M. Reimer, 1994).

The northern half of Area F1 (Figure 12B) contains numerous steam vents. The highest SGCFs within the study area were found within Area F1 , which is consistent with the observed geothermal activity. SGCF in this area range from 13-4490 kg/m^2/yr (mean= 1152 kg/m^2/yr). The origin of these high CO_2 fluxes is probably due to the fact that the SRZ extends from this area of Halemaumau crater possibly forming a fractured zone which allows large amounts of gas to migrate from below to the atmosphere. Area F2 (Figure 12C) encompasses an area which has many visible steam vents scattered within it. The soil here is rocky and it was hard to find suitable sites to perform flux measurements. SGCF values here range from 12-479 kg/m^2/yr (mean= 124 kg/m^2/yr). Area F3 (Figure 12D) is the largest area of the three. As in Area F2, area F3 contains many visible steam vents scattered within it. The crack located in the northeast corner of Figure 12D has many active fumaroles. This area has a large amount of steam issuing from it which explains the high anomalous value (3016 kg/m^2/yr) in this area. SGCFs in Area F3 range from 1-3016 kg/m^2/yr (mean= 130 kg/m^2/yr). In general, SGCFs have a higher mean in Area F1 and about the same mean in areas F2 and F3. The northern part of Area F1 is anomalous when compared with the rest of the study area.

SGCFs were also measured along transects A through I (Figures 10 and 11) wherever a high SGCC was detected by the probe, a flux was measured at the site. Those sites, where soil CO_2 fluxes were taken, are indicated on Figures 9A-9C.

The actual CO_2 fluxes are depicted on Figure 10. Transects E-G (Figure 11) show low values of SGCCs measured by the probe. SGCFs taken along these transects were zero over the sampling time (60-120 seconds). Transects A, B, H and I have high SGCC measured by the probe but low CO_2 flux rates (range= ≤ 2 kg/m^2/yr) (Figure 10). This shows that even though SGCCs are high, CO_2 is not being emitted at a high rate. Transects C and D have high SGCCs and higher fluxes (13 and 38 kg/m^2/yr) at a few sites. These higher SGCCs and fluxes along Transect C are associated with a steaming crack (described in Casadevall and Hazlett, 1983). Transect D has one anomalous value (58 kg/m^2/yr) which cannot be explained here. A soil gas helium survey was conducted by Reimer (1987) very close to transect D. Higher helium values would indicate the presence of magmatic gas. Reimer's (1987) results show no anomalous helium values along Transect D. Therefore, the high SGCF measured along transect D is considered to be uncharacteristic of this area.

SGCF data was plotted against the corresponding SGCC (Figure 14). Some of the fluxes presented here do not have probe samples taken in exactly the same place but those that do were plotted in Figure 14. This graph shows no clear relationship between probe SGCC at depth and CO_2 fluxes at the soil surface. From Figure 14, except for a couple of points, it can be concluded that in general, higher SGCCs at depth do not indicate higher SGCFs at the surface. Rather, higher SGCF measured on the surface usually indicate higher SGCCs at depth throughout the study area. In Figure 14, measurements indicated with SGCC of 3000 ppm are actually greater than 3000 ppm therefore, a correlation between SGCC and SGCF might exist at SGCC

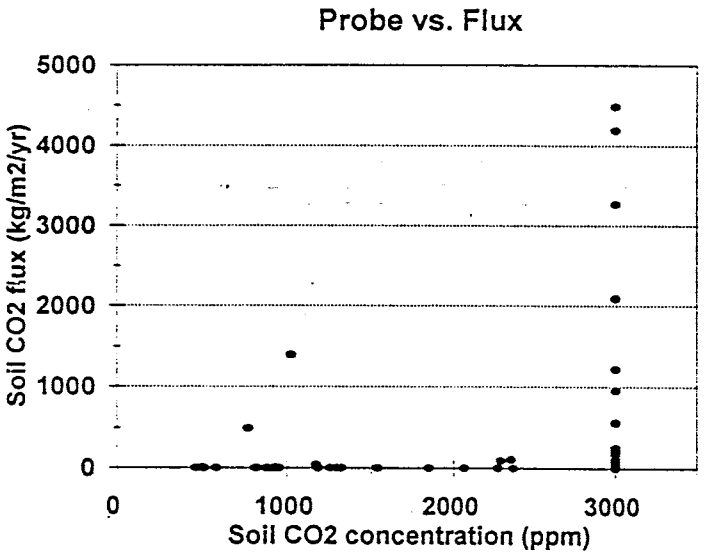

Figure 14. Figure of soil CO_2 concentrations (in ppm) versus CO_2 flux measurements ($kg/m^2/yr$). Carbon dioxide probe and flux measurements were taken at exactly the same sites and this plot represents these points. Soil CO_2 concentrations plotted as 3000 ppm are minimum values.

above 3000 ppm. From the SGCC and SGCF data, it is concluded here that high CO_2 concentrations occur in many different areas at depth but higher CO_2 fluxes occur only within the caldera and a few areas along the SRZ.

Discussion

Source of Soil Gas CO_2 at Kilauea

Elevated SGCC and SGCF in volcanic regions could be produced by a number of factors in addition to volcanic activity, such as microbial activity and vegetation. Soils within the Kilauea caldera and SRZ support little to no vegetation. Microorganisms which produce CO_2 within the soil (Bremner and Blackmer, 1982) have little contribution to the SGCFs and SGCCs (Table 2). The $\delta^{13}C$ data presented in Figure 9 (and Table 3) gives evidence that the gas emitted from the areas measured is derived from a magmatic source at depth. Isotopic measurements of carbon presented in this study generally agree with Halemaumau crater gas data presented by Gerlach and Thomas (1986), Friedman et al. (1987). Two $\delta^{13}C$ values (site 6 and 7, Figure 6) are slightly lower than these magmatic values. It is possible that sample 2 (Figure 7) represents the most pristine (low atmospheric mixing) while sample 5 and 6 represent a higher degree of atmospheric CO_2 mixing which has a $\delta^{13}C$ of about -7 to -8 per mil (Amundson and Davidson, 1990 and Rubin et al., 1987). These two points are considered to have a higher mixing effect associated with them because their $\delta^{13}C$ values do not fall within the measured range at Halemaumau. Site 5 (Figure 6) has a high SGCC (>3000) and a low SGCF (1 kg/m^2/yr). This gas sample

was taken within a sandy arroyo. Due to the $\delta^{13}C$ value of -7.4 per mil at this site, it is thought that this sample could possibly have a higher degree of mixing with the atmosphere (Amundson and Davisson, 1990). Figure 7 also shows that higher SGCFs (>10 kg/m^2/yr) are associated with higher $\delta^{13}C$ values which correspond to a magmatic origin with a smaller degree of atmospheric mixing. Therefore, Site 5 (Figure 6), which has a low flux and lower $\delta^{13}C$, is not considered to be all from a magmatic origin but is a result of mixing with the atmosphere or water at depth. Site 6 (Figure 6) has the same properties as Site 5 but has a slightly higher flux. This sample is very close to Halemaumau crater and is probably a product of higher degrees of atmospheric mixing within the sample. Due to the high SGCC at depth at each of these sites, it is thought that the gas is probably magmatic but has been mixed, to some degree, with the atmosphere.

Numerous cracks, which are exposed to the atmosphere, extend outward from Halemaumau crater. These cracks propagate outward from the walls and probably under many of the sample locations. Atmospheric mixing could occur underneath the Site 6 sample location due to these cracks and the porous nature of the soil. The $\delta^{13}C$ data at site 6 could also be caused by mixing with water at depth or atmospheric contamination during collection.

In general, organic CO_2 production has been ruled out as a cause for contamination of these samples because of the low microbial activity and absence of vegetation. Also, if it is assumed that the $\delta^{13}C$ measurement taken within the nearby fern forest (-21.2 per mil) (Figure 6, Site 7) is indicative of organic activity then these

samples would have much lower $\delta^{13}C$ values. This value, -21.2 per mil, agrees with Rubin et al.'s (1987) range of about -25 to -29 per mil for organic CO_2 from plants around Kilauea. In conclusion, most gas samples collected for carbon isotopic analysis display $\delta^{13}C$ values consistent with derivation from magmatic sources at depth with lower degrees of atmospheric mixing. Lower values of $\delta^{13}C$ can only be attributed to: 1.) larger degrees of atmospheric mixing or 2.) volcanic CO_2 reacting with water at depth.

Factors Affecting Soil CO_2 gas at Kilauea volcano

There are many factors involved when measuring soil CO_2 gas at depth by the probe method and at the surface using the accumulator method. Meteorological factors as well as soil properties affect CO_2 concentration and flux within the soil. No weather measurements were taken during this study period because the equipment needed was not available. Some weather data are available from the Hawaiian Volcanic Observatory (HVO). The problem with HVO's weather data is that it may not apply to the SRZ as there are large variations in rainfall across the region. For example, rainfall measurements taken on the west side and east side of Halemaumau vary by a factor of 2 to 6 (pers. comm. A.J. Sutton, 1994).

Figure 15 illustrates some the factors that might affect both SGCC and SGCF measurements within Kilauea caldera. When using soil probes, CO_2 concentrations may be affected by: 1.) barometric pressure, 2.) air temperature, 3.) relative humidity, 4.) wind speed, 5.) precipitation, 6.) soil temperature and 7.) soil moisture (Reimer, 1980 and Hinkle, 1994). Reimer (1980) found that barometric pressure, soil

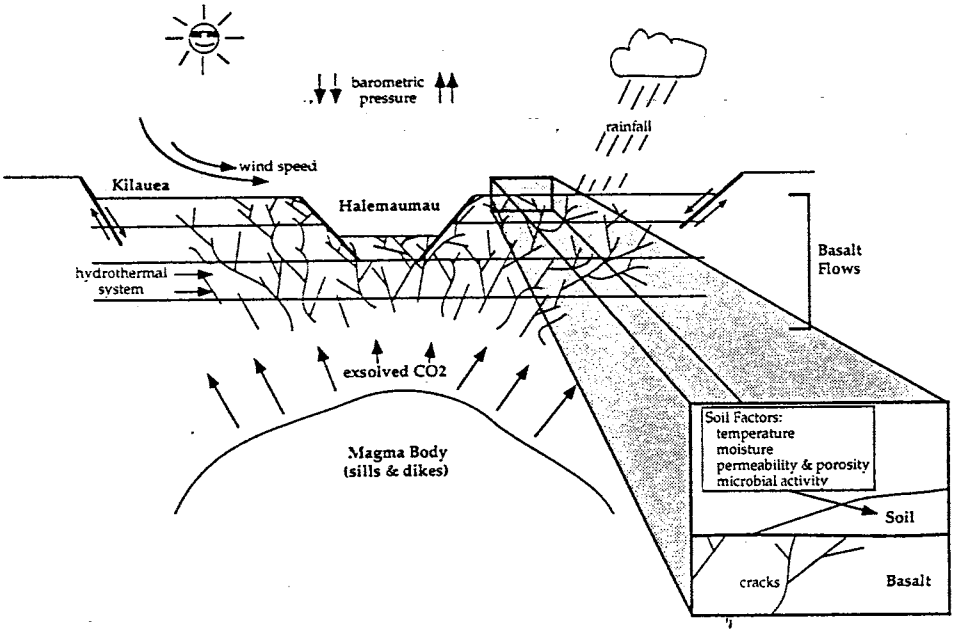

Figure 15. Schematic drawing of a cross-section through Kilauea caldera and Halemaumau crater (not to scale) showing the factors affecting soil CO_2 fluxes and concentrations in the area. Factors include barometric pressure, rainfall, wind speed and direction, faults, cracks within basalt flows, hydrothermal system interaction, and the amount of CO_2 exsolved from the summit magma chamber. Soil factors include: soil temperature, location of cracks underneath the soil, thickness of soil, soil moisture, permeability and porosity and microbial activity within the soil. Cracks within Kilauea caldera are highly exaggerated.

temperature and relative humidity have little effect on helium gas concentrations in the soil. Hinkle (1990 and 1994)) measured soil CO_2 gas at the summit of Kilauea volcano for 13 months using a probe emplaced 0.75 m in the ground. Barometric pressure, soil and air temperatures, relative humidity and rainfall were measured during this study. Hinkle found that barometric pressure and percent relative humidity had no effect on CO_2 concentrations at depth. It was found that rain had the largest impact. High moisture content has a tendency to either flush gases from soil pores or to dissolve these gases. In either case, the result is lower CO_2 concentrations within the soil. Hinkle (1994) reported that increases and decreases of CO_2 concentrations at depth due to soil and air temperatures probably reflects microbial activity in the soil. Microbial activity was reported here as insignificant which leaves rainfall as having the largest impact. Therefore, it is concluded that the probe measurements presented here are a minimum value taking into consideration the affects of rainfall. Wind might also have an effect on CO_2 measurements using the probe method because of the shallow depth (sometimes < 10 cm) and porous nature of the soil at which SGCC were taken. Wind could cause mixing of atmosphere with soil gas which would also yield a minimum value.

Factors affecting SGCF measurements include many of the factors that affect SGCCs. Some factors affecting flux measurements have been studied on radon fluxes from the soil. Schery et al. (1984) studied radon emission from a gravelly sandy loam for three years using the accumulator method and other methods. Their measurements indicate that radon exhalation was dependent on atmospheric pressure variation and

rain.

If the CO_2 emission from magma at depth is relatively constant over the study period, the variation between each standard site and from site to site, suggests that SGCF is controlled by some other physical factor. This factor must control the CO_2 emission rates on a relatively small scale because the sites (B and C) are about 1.5 m away from each other. At Kilauea, atmospheric pressure seemed to have no great variation (0-5 millibars) during each measurement at the standard sites while there was still variation within the standard sites. Rainfall data was collected by the HVO staff and compared with the standard fluxes during the sampling times. There was no correlation between rainfall and the variation of SGCF at each standard site. This is not to say that rain or barometric pressure could not effect SGCF at the standard site. Though it could mean that the standard sites were not measured over a long enough period to deduce any trends between rainfall or barometric pressure. Also, as previously mentioned, the rainfall measurements were taken at HVO and meteorological conditions change rapidly with distance across the summit area.

Due to the poor nature of the soil, the only observed effect on SGCF was the wind. If the soil flux accumulator did not have a good seal with the soil, a gust of wind would make the CO_2 concentration within the box decrease. This was obvious at some locations by the CO_2 concentration displayed on the CO_2 analyzer. When this happened, the accumulator was resealed and another measurement was taken. At many locations this trend was not obvious but it is probable that CO_2 can leak from the accumulator box as shown in Figure 13C and 13D, due to the porous nature and

thickness of the soil encountered in the study area.

Another factor which probably affects SGCC and SGCFS at Kilauea volcano is the location and character of visible cracks at the surface, and cracks underneath the soil (Figure 15). These cracks have formed by inflation at the summit and also from within the basalt flows as they cool. Some of these cracks obviously transport large amounts of steam to the surface while others seem to transport nothing at all. It is unknown how deep these fractures descend.

Thomas and Naughton (1979) found variations of CO_2 and SO_2 concentrations at a 1971 fissure fumarole within Kilauea caldera. They speculated that there is a possible relationship between these gas concentrations and summit inflation. They propose that during times of moderate inflation at the summit, the rock above the chamber is relatively impermeable to most magmatic volatiles and, as the summit inflates, the rock is dilated which causes fractures to open. These fractures provide channelways for the gas to migrate to the surface.

Other factors which were unmeasured or undetected may have a large influence on SGCC and SGCF. Most of the great effects on SGCC and SGCF discussed here decrease the amount of CO_2 (except for large gas emitting cracks). Therefore, all of the SGCCs and SGCFs measured here, are considered minimum values.

Soil CO_2 Flux in Kilauea Caldera

Previously it was concluded that most of the SGCF was being emitted from Area F1, F2 and F3 located within Kilauea caldera. Area F1 (Figure 12B) has the largest CO_2 fluxes of all the areas. Contours in Figure 12B show that most of the

CO_2 degassed is in the northeast corner of the outline in Area F1. The area within each contour was calculated and the fluxes within them were averaged to give a representative CO_2 flux over each area bounded by contours. These were added together in order to calculate the CO_2 flux over the entire area. The results are presented in Table 5. Area F1 has an area of about 109,119 m^2 (0.109 km^2) with a SGCF of approximately 95,800 Mg/yr. Area F2's SGCFs were averaged over the area outlined around the measurements in Figure 12C (Table 5). Area F2 has an area of about 8,125 m^2 with a total SGCF of 1,000 Mg/yr. The same method for Area F1 was used in Area F3 (Figure 12D). Area F3 has an area of about 413,636 m^2 (0.414 km^2) with a total SGCF of 32,000 Mg/yr (Table 5).

It was assumed that the area within Kilauea caldera has similar soil CO_2 degassing as Area F3, with few anomalous CO_2 fluxes. Area F1 was considered anomalous because the high fluxes were not a characteristic of most of the areas studied and therefore not representative of Kilauea caldera. Area F2 was considered too small of an area to integrate these fluxes over the whole caldera. Area F3 is probably most representative of the entire caldera because some areas within it are distant from Halemaumau and have low fluxes. Also, there is only one high anomalous flux measurement located within Area F3. Kilauea caldera seems to have some small areas with higher anomalous fluxes (i.e. Area F1) which must be calculated into the entire CO_2 flux. Even though parts of Area F3 are close to Halemaumau, the CO_2 flux over the entire caldera probably has many areas similar to these parts around Halemaumau judging by the visible steam emitted throughout the

Table 5. Calculated areas of flux measurement areas and CO_2 flux over the area. Flux calculations are described in the text. Area F3 is thought to be most representative of Kilauea caldera. Using Area F3's CO_2 flux and area, Kilauea caldera's total soil CO_2 flux was calculated to be about 2,300 Mg/day.

Area ##	Area(m^2)	CO_2 Flux (Mg/yr)
F1	109,119	95,800
F2	8,125	1,000
F3	413,636	32,010

Total Area of Kilauea caldera= 11 km^2

caldera. Areas with visible steam seem to have a larger SGCF than areas without visible steam.

Kilauea caldera has an area of about 11 km^2. If the flux of 32,000 Mg/y (per 0.414 km^2), from Area F3 (Table 5) is integrated over the area of Kilauea caldera the CO_2 flux is about 850,000 Mg CO_2/yr (Table 5). Therefore, Kilauea caldera, including Halemaumau crater, emits about 2,300 Mg CO_2/day from soil emanations alone (Table 6). It should be noted again that the values used to obtain the CO_2 flux have an estimated error of $\pm$ 35% to $\pm$ 53%. Hinkle and Stokes (1989) measured CO_2, SO_2 and He concentrations at two fumaroles near Halemaumau from 6/17/87 to 2/15/89. One site was on the east side of Halemaumau while the other was located on the 1971 fissure. CO_2/SO_2 ratios at the Halemaumau fumarole ranged from 5.8 to 45.4 with a mean of about 9.0. The 1971 fissure fumarole had CO_2/SO_2 ratios ranging from 0.4 to 6.6 with a mean of about 1.4. The 1971 fissure location was actively depositing sulfur which is not a primary characteristic of the sites in this study. On the other hand, the Halemaumau site is probably more characteristic of the sites measured here and lies within the area in this study. Using the mean CO_2/SO_2 ratio of 9 from the Halemaumau site and COSPEC SO_2 measurements of 87 to 263 Mg SO_2/day (Elias et al, 1993) for Kilauea caldera, gives a CO_2 emission range of about 783 to 2367 Mg CO_2/day (Table 6). Once again, the integrated value of soil CO_2 emission of 2,300 Mg CO_2/day presented here (Table 6), falls into the upper end of this range. If SO_2 is emitted from the soil with CO_2, the COSPEC SO_2 measurements made by Elias et al. (1993) could possibly include soil SO_2 emissions.

Table 6. Calculated soil gas CO_2 and active vent emission rates for Kilauea caldera and Halemaumau crater.

Total CO_2 Emission Rates at Kilauea	
Area F3=	0.414 km^2
Soil CO_2 Flux=	88 Mg/day
Area of Caldera=	11 km^2

Soil gas CO_2 flux at Kilauea (this study)=
2,300 Mg CO_2/day ($\pm$ 35-53%)

CO_2 flux from Halemaumau crater
(calculated from Elias et al., 1993; Hinkle & Stokes, 1989)=
783-2367 Mg CO_2/day

CO_2 flux from Kilauea caldera (this study)=
3100-4700 Mg CO_2/day

CO_2 flux from Kilauea caldera (Gerlach & Graeber, 1985)=
1000-5000 Mg CO_2/day

Therefore, the CO_2 fluxes for Halemaumau presented here, using the COSPEC data combined with the CO_2/SO_2 ratio, could include some CO_2 emitted from the soil. On the other hand, the magnitude of SO_2 concentrations in soil gases and the soil gas SO_2 flux has not been determined. Therefore, most of the SO_2 measured by Elias et al. (1993) is assumed to have originated from Halemaumau crater and sulfur-rich fumaroles within Kilauea caldera and not from soil degassing.

Gerlach and Graeber (1985) calculated a range of CO_2 emission rates for Kilauea caldera, during two-stage degassing, of 1000 to 5000 Mg CO_2/day over July, 1956 to April, 1983 (Table 6). The 2,300 Mg CO_2/day calculated here for soil CO_2 degassing is within this range. Even though the soil CO_2 emission rate includes the area contained within Halemaumau, it is thought that Halemaumau and areas similar to Area F1 (Figure 12B) contribute much larger CO_2 emission rates. Area F1 has an area of about 109,119 m^2 (about 0.1 km^2) with a calculated CO_2 flux of about 95,800 Mg CO_2/yr (Table 5). This area alone produces about 260 Mg CO_2/day. There are obviously areas, similar to Area F1 and within Halemaumau, which are producing high CO_2 emissions but are omitted from the calculated SGCF presented here. But, as previously discussed, Area F3 is thought to be representative of the entire caldera.

As previously mentioned, Reimer (1992) proposed that there is a significant contribution of CO_2 from the areas located around Kilauea caldera (i.e. the SRZ) that could be present during non-eruptive episodes through diffuse soil degassing and that this release is not necessarily through known rifts or active vents. From the data presented here, it seems that the SRZ emits very little CO_2 through soil CO_2 degassing

whereas the areas around Halemaumau crater and within Kilauea caldera emit larger amounts of CO_2 through soil. It seems that much of the degassing within Kilauea caldera is diffuse and leaks out through cracks and weak areas within the rock. Reimer (1992) also estimates that diffuse soil CO_2 emissions are at least equal to that calculated to come from active vents. The estimated CO_2 flux for Kilauea caldera of 2,300 Mg CO_2/day is close to CO_2 (CO_2 emission rate ranges between 783 to 2367 Mg CO_2/day) estimated using COSPEC SO_2 (Elias et al., 1993) data and a CO_2/SO_2 ratio of 9 (Hinkle and Stokes, 1989) (Table 6). It is therefore concluded that as much CO_2 can be emitted from soil CO_2 degassing within Kilauea caldera, as is being emitted from active vents within the caldera.

Gerlach et al. (1991) measured smaller CO_2/SO_2 ratios (Carbon/Sulfur=2) than reported above from fumaroles within Halemaumau crater. They measured gas samples within Halemaumau crater and found Carbon/Sulfur (C/S) ratios of 2 whereas the crater rim fumaroles had C/S of 5 to 16. If the values from Elias et al. (1993) are used with this C/S of 2, and if it is assumed that most of the SO_2 in Kilauea caldera's plume measured by COSPEC originates from within Halemaumau, than CO_2 emissions range from 174 to 526 Mg CO_2/day. These estimates suggest that soil CO_2 degassing within Kilauea caldera accounts for about 4 to 13 times as much CO_2 as emitted from Halemaumau crater.

In general, measurements of fumaroles in and around Kilauea caldera have CO_2/SO_2 ratios greater than 5 (Gerlach and Graeber, 1985; Greenland et al., 1985; Casadevall et al., 1987 and Gerlach et al., 1991). The CO_2/SO_2 measurements of a

summit fumarole within Kilauea caldera made by Hinkle and Stokes (1989) suggest a CO_2/SO_2 mean ratio of about 9. It is assumed here that this is a representative CO_2/SO_2 ratio of most of the gas emitted from this area. Therefore, with the combination of Elias et al. (1993) SO_2 data and a CO_2/SO_2 ratio of 9, the CO_2 flux from Kilauea caldera ranges from 783 to 2367 Mg CO_2/day. The estimated soil CO_2 emission rate is about 2,300 Mg CO_2/day ($\pm$ 35 to 53%). Using the percent errors, this estimate ranges from 1100 to 3500 Mg CO_2/day. Therefore, soil CO_2 gas emissions within Kilauea caldera could equal or be higher than CO_2 emissions inferred from COSPEC data and CO_2/SO_2 ratios (783 to 2367 Mg CO_2/day).

Properties of CO_2 Emanations in Volcanic Soil

Many of the characteristics and properties of volcanic or primary soil CO_2 emissions at other volcanoes have been studied and summarized by Baubron et al. (1991) and Allard (1992). Baubron et al. (1991) outline some of the characteristics and methodology for measuring volcanic soil gas emanations, some of which will be summarized here. Volcanic soil emanations usually lack sulfur compounds and consist primarily of CO_2, with small amounts of hydrogen and rare gases (He, Ar and Rn) which all may be diluted, to some degree, by air. There are three possible sources of soil CO_2 gas: 1.) atmospheric, 2.) carbonate sediments or organic material within volcanic edifices and, 3.) magmatic/mantle sources. Atmospheric contributions are of little importance while the other sources can be distinguished using carbon isotopic ratios ($^{13}C/^{12}C$) (Baubron et al., 1991; Allard, 1992).

Allard (1992) has given an excellent summary of volcanic soil emanations and

their characteristics. Some of these characteristics are briefly stated here: 1.) the degassing is invisible (no vapor plume) and may take place over large areas, 2.) volcanic CO_2 concentrations, at a depth of one meter, can vary from a few percent up to 100% of the gas by volume, 3.) volcanic CO_2 soil concentrations are usually higher than local biogenic CO_2 production, 4.) their emissions can be similar in magnitude to that released by active crater plumes or fumarolic degassing, 5.) they can be the dominant process of degassing and, 6.) ambient atmospheric CO_2 may increase around volcanoes from diffuse volcanic soil emanations. Many of these characteristics apply to Kilauea caldera. Allard (1992) proposed that volcanic CO_2 soil concentrations are usually higher than local biogenic CO_2 production. At Kilauea, volcanic soil CO_2 concentrations are higher than local biological CO_2 production. As Allard (1992) suggested for other volcanoes, the soil degassing at Kilauea is sometimes invisible and takes place over a large area. But most of the degassing seems to occur in areas that do show visible active venting, characterized by water vapor (steam). Allard (1992) also suggested that volcanic soil emanations are sometimes associated with thermal anomalies and fluid circulation in the ground. At Kilauea, it seems that the greater soil CO_2 fluxes are produced in areas where visible steam plumes occur. This suggests that thermal anomalies, possible interaction with hydrothermal activity, and the location of cracks produce larger CO_2 fluxes in these areas. As Allard (1992) and Baubron et al. (1991) proposed, carbon isotopic ratios seem to agree well with measured fumarolic carbon isotopic ratios which suggests a magmatic source for the soil CO_2 concentrations. Allard (1992), Allard et al. (1991)

and Reimer (1992) proposed that diffuse soil CO_2 emissions can sometimes be similar in magnitude to CO_2 emitted from active vents. At Kilauea, it seems that along the SRZ, outside of the caldera, there is not a great amount of CO_2 being emitted. However, within the caldera, large amounts of CO_2 are being emitted especially around active fumaroles or vents. These soil CO_2 emissions seem to be similar in magnitude than emissions from Halemaumau.

Soil CO_2 emanations measured at Kilauea do not necessarily fall directly under Allard's (1992) definition of diffuse soil emanations because Kilauea caldera is essentially an active vent. The higher soil CO_2 emissions measured at Kilauea are not located on the flanks of Kilauea although higher SGCFs could exist in areas outside this study area. Other areas on the flanks of Kilauea could be emitting CO_2 in a diffuse manner. The data presented here suggests that CO_2 and possibly other gases can escape through large portions of calderas, rather than at visibly active fumaroles or vents within the caldera, and that rift zones, extending from the caldera, do not necessarily provide a path for gases to escape unless there is a magmatic input associated with them.

Baubron et al. (1991) suggested that areas of high CO_2 flux might be a criteria for selection of gas monitoring sites around volcanoes. Within Kilauea caldera, the highest CO_2 emission rates were measured on the west side of Halemaumau (Area F1, Figure 12B) probably near the junction of the SRZ and Halemaumau. This area would probably provide a good location for the monitoring of CO_2 emissions. These data could be used in conjunction with summit inflation measurements and SO_2

measurements to infer the timing, and possible to estimate the amount, of magma supplied to the summit chamber. Further investigations of soil CO_2 emissions at the summit should include meteorological measurements very close to the sampling sites and, the installation of a permanent CO_2 flux station in order to monitor the variations through time. The ideal study for monitoring changes in magma supply to Kilauea's summit reservoir would allow a comparison between meteorological conditions (i.e. rainfall, wind speed and direction, barometric pressure), summit inflation, SO_2 and CO_2 emissions (and possibly other gases, i.e. helium).

Comparisons with Volcanoes, Global Volcanism and Anthropogenic CO_2 Emissions

Using the soil CO_2 emission rate, 2300 Mg CO_2/day ($\pm$35 to 53%), combined with the range of CO_2 measured in the plume, 783 to 2367 Mg CO_2/day, gives an estimated flux for Kilauea's summit of about 3100 to 4700 Mg CO_2/day or a minimum of 1.1×10^6 Mg CO_2/yr (Table 6). This falls within the calculated emission rate range of 1000 to 5000 Mg CO_2/day (Gerlach and Graeber, 1985) for July 1956 to April 1983 at Kilauea's summit (Table 6). When compared with volcanoes such as Mt. Etna, the amount of CO_2 degassed by Kilauea is nominal (Table 7). Mt. Etna releases more than 70,000 Mg CO_2/day from its crater alone (Allard et al., 1991). This is about 15 times the amount Kilauea is estimated to emit here. Mt. Etna probably emits more CO_2 than Kilauea and many other volcanoes because it resides over an alkaline basaltic magma which contains larger abundances of CO_2 (Allard et al., 1991) than Kilauea's tholeiitic basalt magma. Mt. Etna might also release larger amounts of soil gas CO_2 because of the morphology of its magma body and cone. Mt. Etna's magma

Table 7. Carbon dioxide emissions from active vents and through soils at Kilauea and other volcanoes.

CO_2 Emissions from Volcanoes (in Mg CO_2/day)		
Volcano	**Active Vents**	**Soil CO_2 Emissions**
Kilauea	783-2367	2,300
Mt. Etna	70,000	55,000
Vulcano	180	30
White Isl.	3,562	----

Table 8. Global volcanic CO_2 emissions calculated by other authors.

Global Volcanic CO_2 Emissions (in Mg CO_2/day)	
CO_2	**Author**
$3x10^5$	Marty & Le Cloarec (1992)
$4x10^5$	Gerlach (1991)
$3X10^5$	Le Cloarec & Marty (1990)
$3.3x10^5$	Mean
$5.5x10^7$	Anthropogenic (Leavitt, 1982)

body probably has a more defined conduit than Kilauea's summit caldera which is thought to be a dike and sill complex. Also, Mt. Etna is a stratovolcano which has steeper slopes than of Kilauea's shield. Therefore, it is possible that a more defined magma body centered under a steeper cone, like Mt. Etna, might be able to emit more of its CO_2 through its flanks than a poorly defined magma body under a broad shield volcano.

Using airborne COSPEC measurements and fumarole samples, Rose et al. (1986) estimated a CO_2 output for White Island Volcano, New Zealand of approximately 3,562 Mg CO_2/day during November, 1983 (Table 7). These measurements were characterized by a quiescent plume prior to the December, 1983 eruption (Rose et al., 1986). The Kilauea CO_2 degassing rate calculated here is of the same magnitude as White Island although Rose et al. (1986) reported an emission rate of 822 Mg CO_2/day in November, 1984. Harris et al. (1981) reported means ranging from 5,300 to 11,500 Mg CO_2/day for the period of July through October, 1980 at Mt. St. Helens. Their data was collected from the plume by airborne techniques. In comparison to Kilauea, Mt. St. Helens emitted more CO_2 per day during these times.

Using different means, several authors have attempted to quantify the total amount of CO_2 emitted from global volcanism. Marty and Le Cloarec (1992) calculated that global volcanism accounts for 1.1×10^8 Mg CO_2/yr while Gerlach (1991) calculated a CO_2 flux of about 1.54×10^8 Mg CO_2/yr (Table 8). Le Cloarec and Marty (1990) calculated a global volcanic CO_2 emission rate of about 1.07×10^8 Mg CO_2/yr (Table 8). In general, these CO_2 emission rates all have the same magnitude with a

mean of about 1.24×10^8 Mg CO_2/yr contributed by global volcanism. Kilauea's summit minimum estimate of CO_2 output calculated here makes up about 0.9% of the total CO_2 output by global volcanism. This is a very small contribution. Anthropogenic CO_2 emissions are on the order of 2×10^{10} Mg CO_2/yr (Leavitt, 1982) (Table 8) which is about 160 times greater than CO_2 emitted from global volcanism.

Conclusions

Carbon dioxide measurements in this study were taken when Kilauea caldera was emitting chamber gas composed primarily of CO_2 (Gerlach and Graeber, 1985; Greenland et al., 1985). The active vent, Pu'u O'o, continued to emit gas and an active lava lake throughout the study period. Gerlach (1986) proposed that as magma rises underneath Kilauea caldera, much of the CO_2 contained is exsolved at greater depths (about 1 km, 10MPa) than SO_2 and H_2O. It is probable that this CO_2 will be the first gas vented into the atmosphere and provides a source for the CO_2 emitted through soils at the surface. The organic CO_2 contribution is considered to be negligible in the study area while a direct correlation between higher $\delta^{13}C$ (>-5 per mil) values and higher CO_2 flux suggests a magmatic source with minimal atmospheric mixing for most of the soil gas. Two gas samples show evidence of larger degrees of mixing with an atmospheric component or possibly hydrothermal areas at depth.

The migration of CO_2 from the magma chamber to the atmosphere is affected by meteorologic factors and the nature of the channelway. Effects of the more important meteorologic factors (rain and wind) on both soil probe and soil flux

measurements would tend to result in a minimum value. In the future, meteorologic factors near each sampling site need to be monitored due to the great meteorological variations present across Kilauea summit area and caldera. Cracks within the summit area seem to transport large amounts of gas while in other locations they do not. It is assumed in this study that the rapid migration of CO_2 through soils is controlled by these cracks and is dominated by mass transportation processes rather than diffusion. It is difficult to perform soil gas surveys around Halemaumau and in the SRZ due to the limited amount, thickness and porous nature of the soil. While rates of soil CO_2 emission can be measured using the accumulator method, the percent error is large.

Soil CO_2 probe concentrations were used to locate areas of CO_2 degassing. Around Halemaumau crater and most of the SRZ transects, there are relatively high concentrations (>500 ppm) of CO_2 at depths ranging from 5 to 85 cm. In some instances, the proximity to cracks with visible steam correlated with the CO_2 concentrations, but this was not generally the case. It is concluded that higher soil CO_2 concentrations (3000 ppm or less) at depth do not indicate high CO_2 fluxes at the surface. But, higher CO_2 fluxes usually indicate higher CO_2 concentrations at depth.

The slopes of soil CO_2 emissions over time were, in general, highly linear using the accumulator method. From measurements at the standard sites it is concluded that CO_2 emissions vary greatly on a small scale (meters) from place to place. The highest CO_2 emissions were found in the northern half of Area F1 (Figure 12B). There is a large amount of visible steam in this area which is probably a function of fractures created by the intersection of the SRZ and Halemaumau. Area

F1 is considered anomalous when compared with the rest of the study area. Areas F2 and F3 (Figure 12) also have smaller steam vents scattered throughout but CO_2 fluxes were lower than in Area F1. In general, it is concluded that areas with the highest CO_2 fluxes were associated with visible steam.

Soil CO_2 fluxes along the SRZ are lower than those within Kilauea caldera. A few sites (like along transect C, Figure 10C) have higher CO_2 concentrations and fluxes but these are associated with active steaming from nearby cracks. Higher CO_2 concentrations occur in many different areas at depth but higher CO_2 fluxes mostly occur within Kilauea caldera and very few exist along the SRZ. Therefore, within the study area, most CO_2 degassed by Kilauea enters the atmosphere within the caldera, and especially in and around Halemaumau crater.

Assuming that Area F3 (Figure 12D) has similar soil CO_2 degassing rates as all of Kilauea, the entire area of the caldera (about 11 km^2) emits about 2,300 ($\pm$ 35 to 53%) Mg CO_2/day from soil emissions alone. Using a CO_2/SO_2 ratio of 9 and SO_2 COSPEC data, Halemaumau crater emits about 783 to 2367 Mg CO_2/day. It is concluded that soil CO_2 emissions within the caldera are at least equal to that calculated to come from Halemaumau crater assuming that the COSPEC SO_2 data is from Halemaumau alone. Other unmeasured areas on the flanks of Kilauea could be emitting CO_2 through the soil.

It is concluded that CO_2 escapes through large portions of calderas, rather than just at visibly active fumaroles within the caldera, and that rift zones extending from the caldera do not necessarily provide a path for CO_2 to escape unless there is a

magmatic input associated with it. The combined total estimated flux for the summit of Kilauea ranges from 3100 to 4700 Mg CO_2/day which contributes a small amount (0.9%) of CO_2 compared to the total CO_2 output by global volcanism.

References

Allard P (1992) Diffuse Degassing of Carbon Dioxide Through Volcanic Systems: Observed Facts and Implications. Rept Geol Surv Japan 279:7-11

Allard P, Carbonelle J, Dajlavic D, Le Bronec J, Morel P, Robe MC, Maurenas JM, Faivre-Pierret R, Martin D, Sabroux JC, Zettwoog P (1991) Eruptive and diffuse emissions of CO_2 from Mount Etna. Nature 351:387-391

Amundson RG, Davidson EA (1990) Carbon dioxide and nitrogenous gases in the soil atmosphere. Journal of Geochemical Exploration 38:13-41

Anderson AT (1975) Some basaltic and andesitic gases. Rev Geophys Space Phys 13:37-55

Anderson JPE (1982) Soil Respiration. Methods of Soil Analysis, Part 2 Chemical and Microbiological Properties-Agronomy Monograph no. 9 (2nd Edition):831-871

Baubron JC, Allard P, Toutain JP (1990) Diffuse volcanic emissions of carbon dioxide from Vulcano Island, Italy. Nature 344:51-53

Baubron JC, Allard P, Sabroux JC, Tedesco D, Toutain JP (1991) Soil gas emanations as precursory indicators of volcanic eruptions. Journal of the Geological Society, London 148:571-576

Bremner JM, Blackmer AM (1982) Composition of Soil Atmospheres. Methods of Soil Analysis, Part 2 Chemical and Microbiological Properties-Agronomy Monograph no. 9 (2nd Edition):873-901

Casadevall TJ, Hazlett RW (1983) Thermal Areas on Kilauea and Mauna Loa Volcanoes, Hawaii. J Volcan Geotherm Res 16:173-188

Casadevall TJ, Stokes JB, Greenland LP, Malinconico LL, Casadevall JR, Furukawa BT (1987) SO_2 and CO_2 emission rates at Kilauea volcano, 1979-1984. USGS Prof Paper 1350:771-780

Cox ME (1983) Summit Outgassing as Indicated by Radon, Mercury and pH Mapping, Kilauea Volcano, Hawaii. J Volcan Geotherm Res 16:131-151

Dvorak JJ, Okamura AT (1987) A hydraulic model to explain variations in summit tilt rate at Kilauea and Mauna Loa Volcanoes. USGS Prof Paper 1350:1281-1296

Dzurisin D, Koyanagi RY, English TT (1984) Magma supply and storage at Kilauea Volcano, Hawaii, 1956-1983. J Volcan Geotherm Res 21:177-206

Elias T, Sutton AJ, Stokes JB (1993) Current SO_2 Emissions at Kilauea Volcano: Quantifying Scattered Degassing Sources. AGU Fall Meeting 1993:670

Ellsworth WL, Koyanagi RY (1977) Three-Dimensional Crust and Mantle Structure of Kilauea Volcano, Hawaii. J Geophys Res 82:5379-5394

Friedman I, Gleason J, Jackson T (1987) Variation of $\delta^{13}C$ in fumarolic gases from Kilauea Volcano. USGS Prof Paper 1350 1:805-807

Gerlach TM (1982) Interpretation of Volcanic Gas Data from Tholeiitic and Alkaline Mafic Lavas. Bull Volcanol 45-3:235-244

Gerlach TM (1986) Exsolution of H_2O, CO_2, and S during eruptive episodes at Kilauea volcano, Hawaii. J Geophys Res 91:12,177-12,185

Gerlach TM (1991) Present-day CO_2 emissions from Volcanos. EOS 72:249, 254-255

Gerlach TM, Graeber EJ (1985) Volatile budget of Kilauea volcano. Nature 313:273-277

Gerlach TM, Thomas DM (1986) Carbon and sulphur isotopic composition of Kilauea parental magma. Nature 319:480-483

Glinski J, Stepniewski W (1985) Chapter 3: Soil Air. In: Soil Aeration and Its Role for Plants. CRC Press

Greenland LP, Rose WI, Stokes JB (1985) An estimate of gas emissions and magmatic gas content from Kilauea volcano. Geochim Cosmochim Acta 49:125-129

Harris DM, Sato M, Casadevall TJ, Rose WI, Bornhorst TJ (1981) Emission rates of CO_2 from plume measurements. USGS Prof Pap 1250:201-207

Heliker CC, Wright TL (1991) The Pu'u'O'o-Kupaianaha eruption of Kilauea. EOS 47:521, 526, 530

Hinkle ME (1990) Tabulation of N_2, O_2, CO_2 and He Concentrations in Soil Gases Collected Regularly for 13 Months at a Site on the Summit of Kilauea Volcano. USGS Open File Report 90-661:1-19

Hinkle ME (1994) Environmental conditions affecting concentrations of He, CO_2, O_2 and N_2 in soil gases. Applied Geochem 9:53-63

Hinkle ME, Stokes JB (1989) Tabulation of CO_2, SO_2 and He Concentrations in Summit Fumarole Gases and Wind and Rainfall Data at Kilauea Volcano, Hawaii, for the Period June 1987 - February 1989. USGS Open File Report 90-507:1-27

Holcomb RT (1987) Eruptive history and long-term behavior of Kilauea volcano. USGS Prof Paper 1350:261-350

Kanemasu ET, Powers WL, Sij JW (1974) Field Chamber Measurements of CO_2 Flux from Soil Surface. Soil Science 118:233-237

Leavitt SW (1982) Annual volcanic carbon dioxide emission: An estimate from eruption chronologies. Environ Geol 4:15-21

Le Cloarec MF, Marty B (1990) Volatile fluxes from volcanoes. Terra Nova 3:17-27

Marty B, Le Cloarec MF (1992) Helium-3 and CO_2 fluxes from subaerial volcanoes estimated from polonium-210 emissions. J Volcan Geotherm Res 53:67-72

Mattox TN, Heliker C, Kauahikaua J, Hon K (1993) Development of the 1990 Kalapana Flow Field, Kilauea Volcano, Hawaii. Bull Volcanol 55:407-413

McCarthy HJ, Reimer MG (1986) Advances in Soil Gas Geochemical Exploration for Natural Resources: Some Current Examples and Practices. J Geophys Res 91:12327-12338

McPhie J, Walker GPL, Christiansen RL (1990) Phreatomagmatic and phreatic fall and surge deposits from explosions at Kilauea volcano, Hawaii, 1790 A.D.: Keanakakoi Ash Member. Bull Volcanol 1990:334-354

Moore RB, Trusdell FA (1993) Geology of Kilauea Volcano. Geothermics 22:243-254

Pan V, Holloway JR, Hervig RL (1991) The pressure and temperature dependence of carbon dioxide solubility in tholeiitic basalt melts. Geochim Cosmochim Acta 55:1587-1595

Peterson DW (1967): Geologic map of the Kilauea Quadrangle, Hawaii. U.S.G.S., Washington D.C. . Scale 1:24,000.

Reimer GM (1980) Use of Soil-Gas Helium Concentrations for Earthquake Prediction: Limitations Imposed by Diurnal Variation. J Geophys Res 85:3107-3114

Reimer GM (1987) Helium at Kilauea Volcano, Part II: Distribution in the Summit Region. USGS Prof Paper 1350:815-819

Reimer GM (1990) Reconnaissance Techniques for Determining Soil-Gas Radon Concentrations: An Example from Prince Georges County, Maryland. Geophys Res Lett 17:809-812

Reimer GM (1992) Soil-Gas Flux of CO_2 From Non-Venting Areas of the Kilauea Summit, Hawaii. EOS Fall Meeting:708

Rose WI, Chuan RL, Giggenbach WF, Kyle PR, Symonds RB (1986) Rates of sulfur dioxide and particle emissions from White Island volcano, New Zealand, and an estimate of the total flux of major gaseous species. Bull Volcano 48:181-188

Rubin M, Lockwood JP, Friedman I (1987) Effects of volcanic emanations on carbon-isotope content of modern plants near Kilauea volcano. USGS Prof Paper 1350:209-211

Ryan MP, Koyanagi RY, Fiske RS (1981) Modeling the Three-Dimensional Structure of Macroscopic Magma Transport Systems: Application to Kilauea Volcano, Hawaii. J Geophys Res 86:7111-7129

Schery SD (1989) The Design of Accumulators and Their Use in Determining the Radon Availability of Soil. Air & Waste Management Association 82nd Annual Meeting, June 25-30:1-9

Schery SD, Gaeddert DH, Wilkening MH (1984) Factors Affecting Exhalation of Radon From a Gravelly Sandy Loam. J Geophys Res 89:7299-7309

Schneider SH (1989) The Greenhouse Effect: Science and Policy. Science 243:771-781

Stolper E, Holloway JR (1988) Experimental determination of the solubility of carbon dioxide in molten basalt at low pressure. Earth Planet Sci Lett 87:397-408

Swanson DA, Duffield WA, Fiske RS (1976) Displacement of the South Flank of Kilauea Volcano: The Result of Forceful Intrusion of Magma Into the Rift Zones. USGS Prof Paper 963:1-39

Thomas DM, Naughton JJ (1979) Helium/Carbon Dioxide Ratios as Premonitors of Volcanic Activity. Science 204:1195-1196

U.S. Dept. of Agriculture (1973) Soil survey of the Island of Hawaii, State of Hawaii. Soil Conservation Service, US Dept of Agriculture, Washington, DC:1-115

Wilkening M (1990) Radon- Soil to Air. In: Wilkening M (ed) Radon in the Environment. Elsevier

Wright TL (1984) Origin of Hawaiian Tholeiite: A Metasomatic Model. J Geophys Res 89:3233-3252

Appendix A: Maps showing location of soil gas CO_2 concentrations around Halemaumau crater and along the Southwest Rift Zone transects. Numbers in parenthesis along the transects are soil gas CO_2 flux measurement sites (flux can be found in Appendix B). Each map is followed by the data for each of the sites. All soil gas CO_2 concentrations are in ppm.

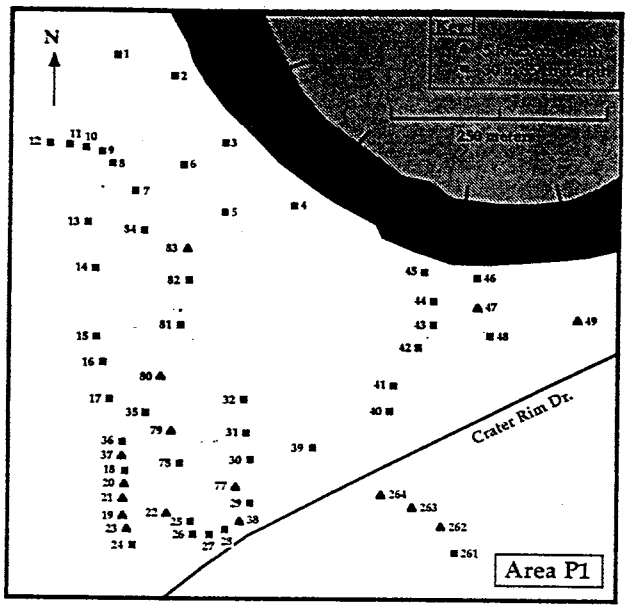
N
Crater Rim Dr.
Area P1

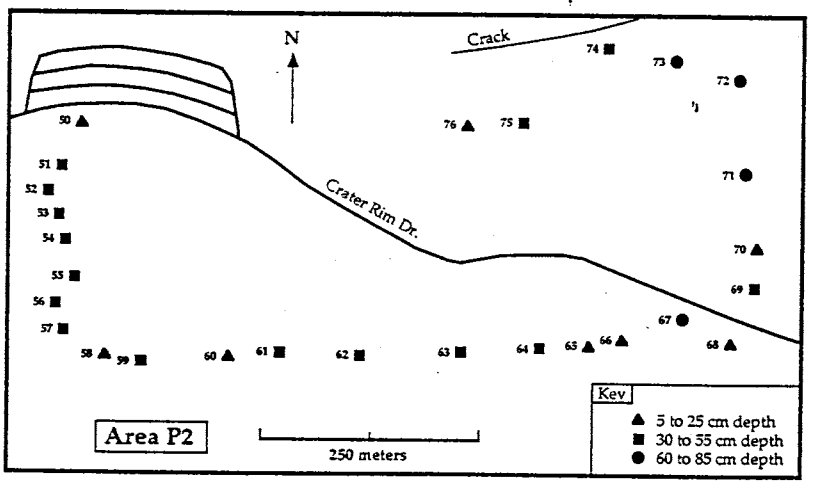
N
Crack
Crater Rim Dr.
Area P2
250 meters
Key
5 to 25 cm depth
30 to 55 cm depth
60 to 85 cm depth

APPENDIX A

Soil Gas CO2 Concentration and Depth Data at Kilauea Volcano

Note: SGCC= Soil Gas CO2 Concentration

DATE / AREA / SITE #	SGCC	DEPTH in cm
07/26/93 AREA P1		
1	>3000	40
2	>3000	40
3	1018	40
4	570	35
5	1880	55
6	768	40
7	>3000	55
8	>3000	40
9	>3000	40
10	>3000	40
11	>3000	40
12	>3000	40
13	>3000	40
14	>3000	55
15	>3000	40
16	>3000	55
17	>3000	55
18	>3000	55
19	606	25
20	>3000	25
21	>3000	25
22	1384	25
23	864	25
24	571	40
25	590	55
26	532	55

DATE / AREA / SITE #	SGCC	DEPTH in cm
07/26/93 AREA P1		
29	530	40
30	540	55
31	>3000	55
32	>3000	40
35	>3000	40
36	>3000	40
37	>3000	25
38	794	25
07/27/93 AREA P1		
39	451	55
40	477	40
41	494	55
42	747	40
43	2293	40
44	2351	40
45	450	55
46	425	40
47	>3000	25
48	>3000	40
49	802	25

DATE / AREA / SITE #	SGCC	DEPTH in cm
08/01/93 AREA P2 except for site #77		
50	>3000	25
51	>3000	30
52	>3000	30
53	1049	40
54	764	30
55	550	30
56	557	30
57	507	30
58	506	25
59	506	30
60	811	25
61	502	40
62	>3000	30
63	1163	30
64	>3000	40
65	2405	25
66	>3000	25
67	>3000	60
68	2269	25
69	>3000	30
70	>3000	25
71	1935	75
72	>3000	75
73	932	85
74	2286	65
75	>3000	55

DATE / AREA / SITE #	SGCC	DEPTH in cm
08/04/93 AREA P1		
78	623	30
79	553	25
80	441	25
81	488	50
82	>3000	40
83	>3000	25
84	>3000	55

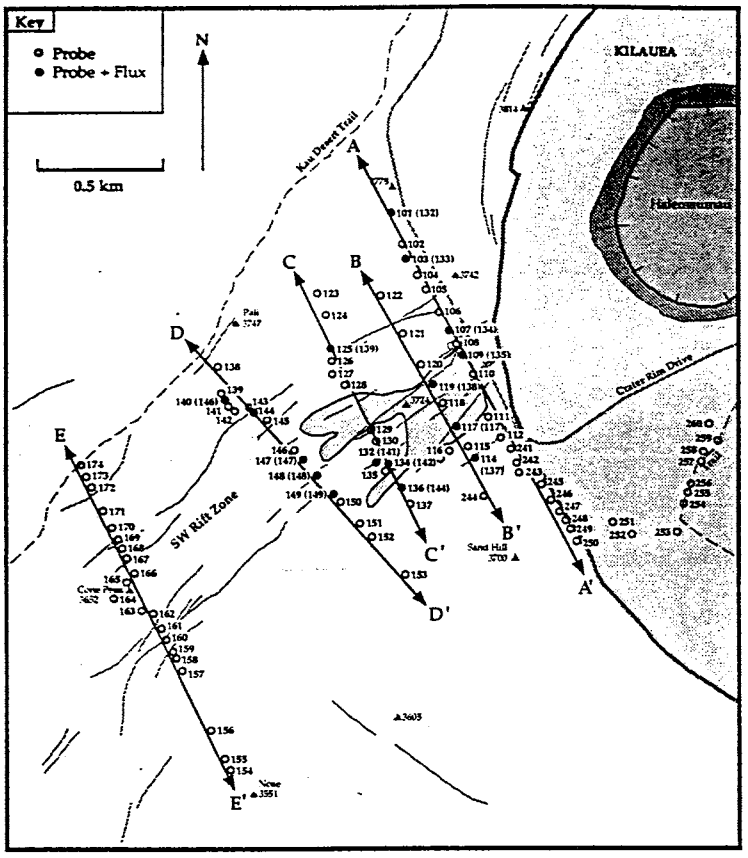
Key
Probe
Probe + Flux
N
0.5 km
KILAUEA
Kau Desert Trail
Crater Rim Drive
SW Rift Zone
Sand Hill
A
A'
B
B'
C
C'
D
D'
E
E'

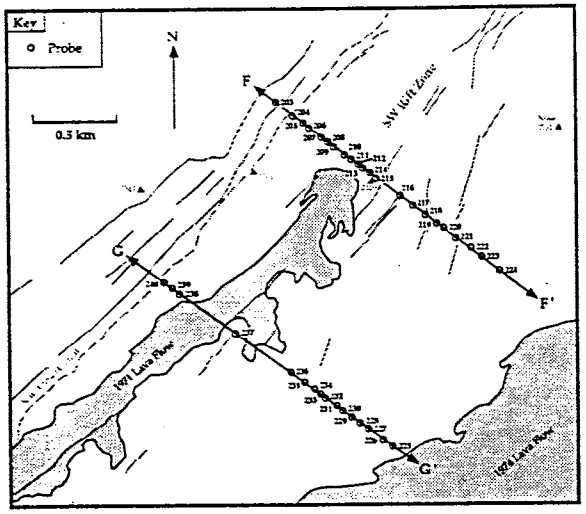
Key
Probe
N
0.5 km
F
F'
G
G'
SW Rift Zone
1971 Lava Flow
1974 Lava Flow

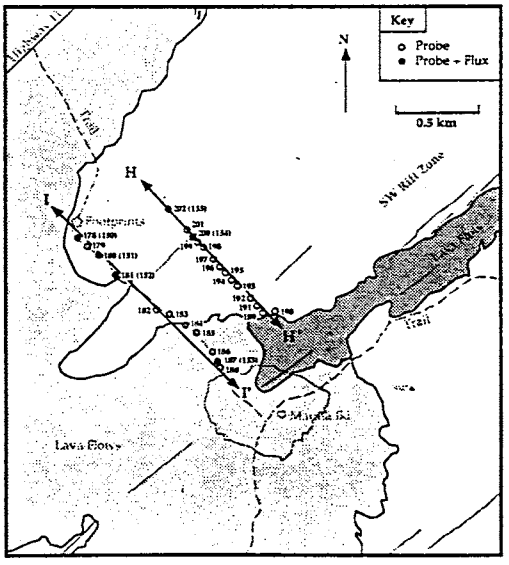
Key
Probe
Probe + Flux
N
0.5 km
H
H'
I
I'
SW Rift Zone
Trail
Lava flows

APPENDIX A (CONT.)

DATE AREA SITE #	SGCC	DEPTH in cm
08/06/93		
TRANSECT A		
101	1038	55
102	491	10
103	917	85
104	750	85
105	432	85
106	437	25
107	1291	10
108	1089	85
109	935	10
110	489	10
111	401	25
112	>3000	75
241	438	55
242	433	55
243	314	25
245	386	35
246	395	20
247	390	20
248	442	65
249	384	60
250	388	40

DATE AREA SITE #	SGCC	DEPTH in cm
08/06/93		
TRANSECT B		
122	577	25
121	1242	20
120	1566	85
119	>3000	15
118	>3000	85
117	424	20
116	954	55
115	>3000	55
114	>3000	55
244	395	55

DATE AREA SITE #	SGCC	DEPTH in cm
08/07/93		
TRANSECT C		
123	389	85
124	376	85
125	1340	85
126	915	85
127	369	25
128	633	85
129	>3000	85
130	1189	10
132	>3000	40
134	>3000	55
135	1845	25
136	>3000	25
137	1308	55

DATE AREA SITE #	SGCC	DEPTH in cm
08/08/93		
TRANSECT D		
138	622	70
139	876	70
140	933	75
141	576	85
142	375	75
143	377	85
144	389	25
145	464	40
146	>3000	10
147	>3000	20
148	1539	85
149	1250	25
150	1045	55
151	169	85
152	341	55
153	360	25

APPENDIX A (CONT.)

DATE AREA SITE #	SGCC DEPTH in cm	
08/08/93		
TRANSECT E		
174	355	75
173	397	60
172	349	25
171	387	65
170	240	85
169	390	25
168	130	60
167	103	85
166	380	85
165	320	85
164	380	85
163	375	25
162	362	25
161	382	50
160	406	50
159	395	25
158	380	55
157	498	55
156	417	35
155	509	15
154	420	25

DATE AREA SITE #	SGCC DEPTH in cm	
08/09/93		
TRANSECT I		
178	945	85
179	1343	75
180	1319	50
181	2364	75
182	1680	85
183	564	10
184	473	40
185	701	20
186	530	20
187	1176	55
188	388	40

DATE AREA SITE #	SGCC DEPTH in cm	
08/09/93		
TRANSECT H		
202	>3000	60
201	1481	55
200	2064	55
199	437	40
198	850	55
197	452	25
196	640	25
195	640	15
194	375	85
193	653	35
192	665	10
191	479	20
189	378	25
190	200	60

DATE AREA SITE #	SGCC DEPTH in cm	
08/10/93		
TRANSECT F		
203	300	85
204	302	70
205	417	25
206	380	25
207	425	35
208	385	35
209	435	15
210	415	10
211	360	25
212	376	70
213	539	10
214	385	50
215	490	15
216	402	20
217	420	10
218	365	85
219	375	85
220	380	85
221	334	85
222	382	25
223	289	85
224	258	85

APPENDIX A (CONT.)

DATE AREA SITE #		SGCC DEPTH in cm
08/10/93		
TRANSECT G		
240	**370**	**25**
239	**298**	**55**
238	**365**	**55**
237	**330**	**85**
236	**352**	**85**
235	**283**	**85**
234	**379**	**25**
233	**287**	**50**
232	**316**	**50**
231	**230**	**20**
230	**365**	**85**
229	**420**	**10**
228	**346**	**55**
227	**377**	**25**
226	**393**	**10**
225	**312**	**65**

DATE AREA SITE #		SGCC DEPTH in cm
08/11/93		
East of TRANSECT A		
251	**390**	**25**
252	**389**	**10**
253	**377**	**15**
254	**391**	**50**
255	**388**	**15**
256	**500**	**55**
257	**394**	**10**
258	**395**	**15**
259	**407**	**10**
260	**436**	**10**

Appendix B: Maps showing the location of soil gas CO_2 flux (SGCF) measurements around Halemaumau. SGCF measurement sites along the Southwest Rift Zone transects are located in Appendix A. The maps are followed by a set of graphs corresponding to the CO_2 at each site. Dark lines on each graph are linear regression lines. All CO_2 fluxes calculated from the slope of the line and given on the graphs are in $kg/m_2/year$.

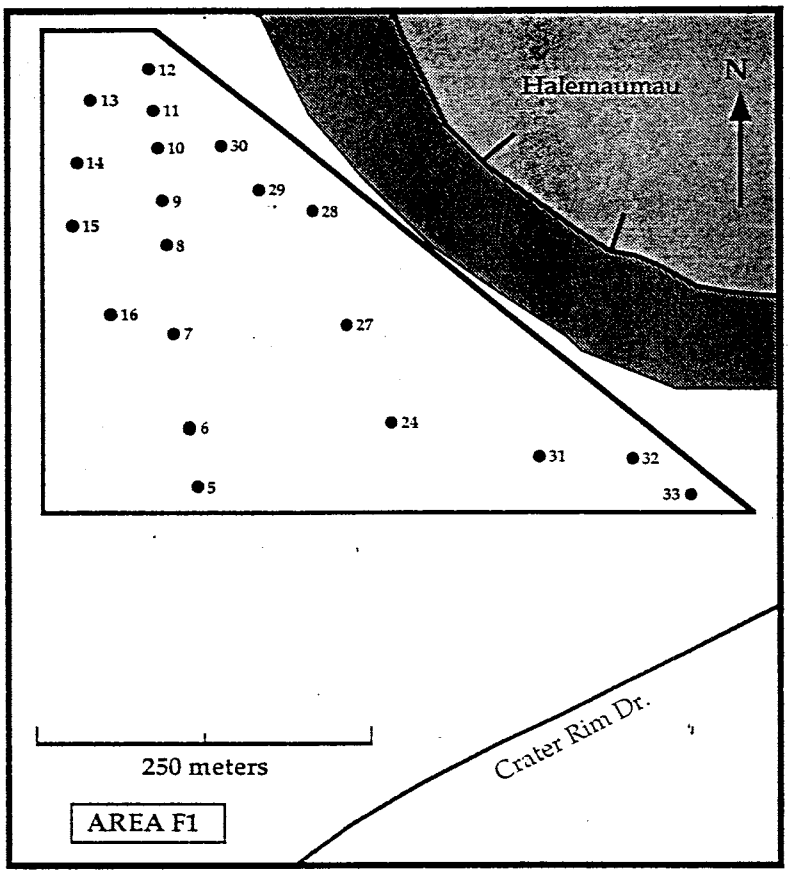
Halemaumau
N
12
13
11
10
30
14
29
9
28
15
8
16
7
27
6
24
31
32
5
33
250 meters
Crater Rim Dr.
AREA F1

Graphs corresponding to the CO_2 flux at sites within Area F1.

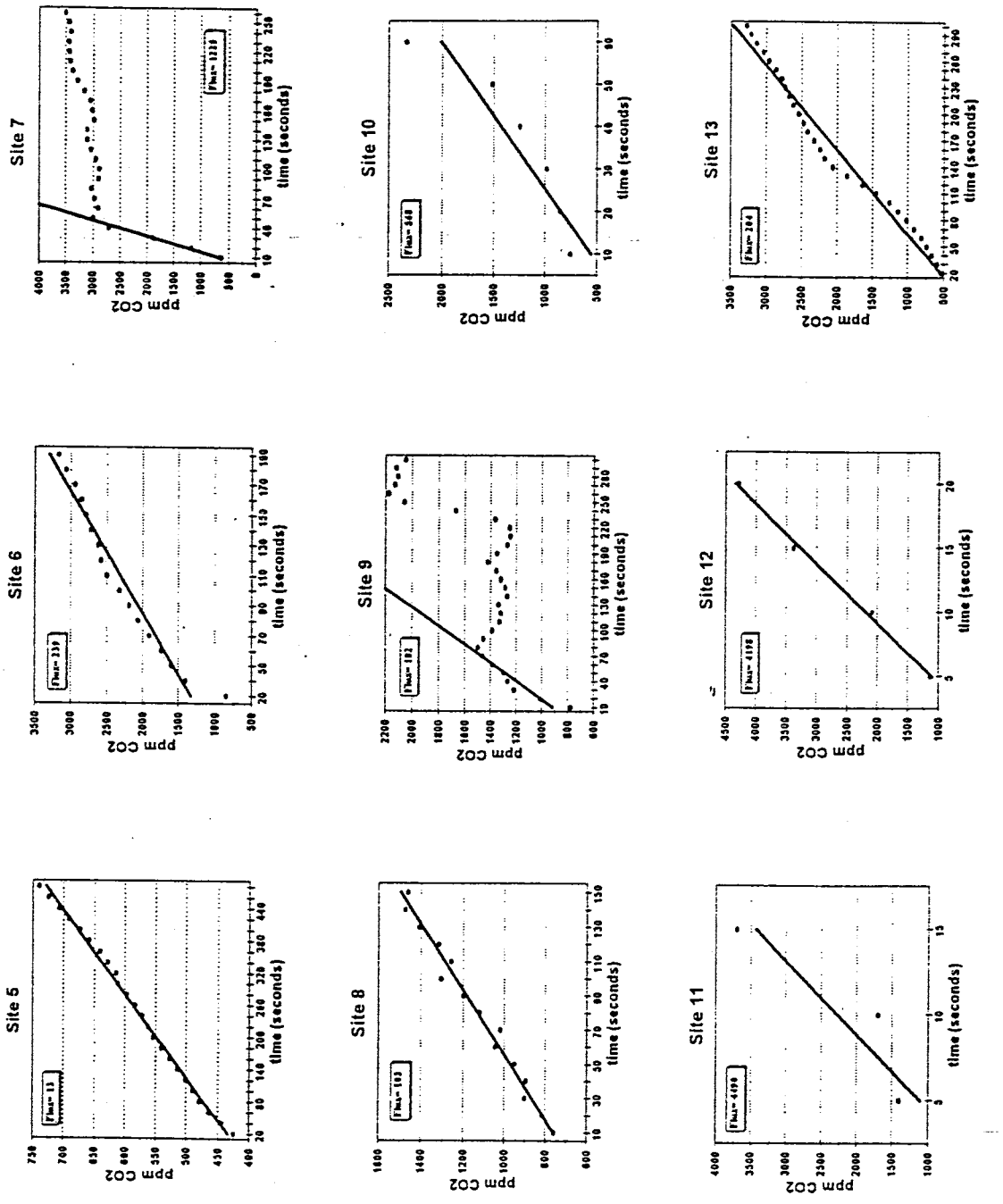

Graphs corresponding to the CO_2 flux at sites within Area F1.

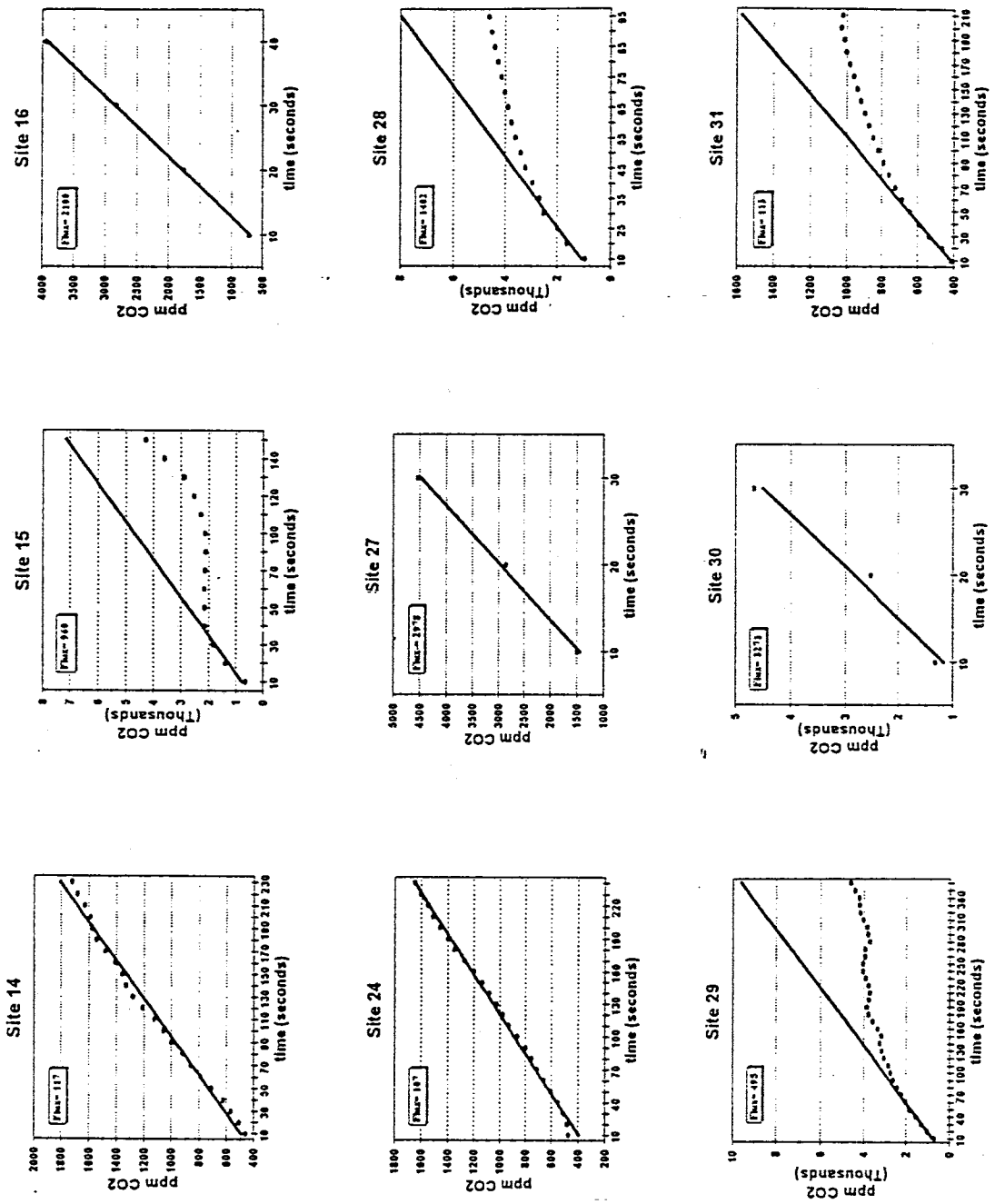

Graphs corresponding to the CO_2 flux at sites within Area F1.

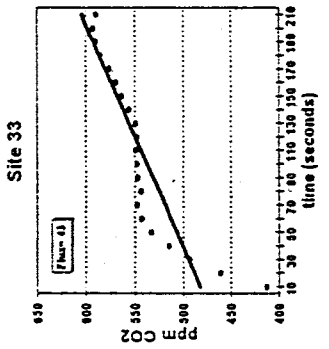

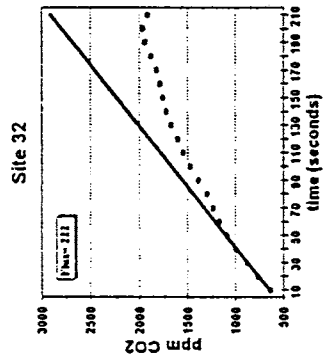

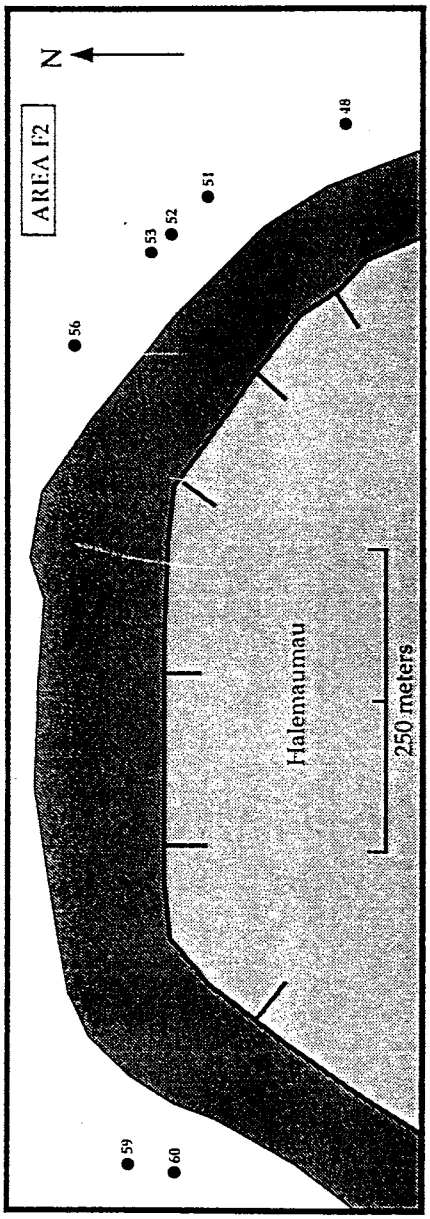
N
AREA F2
48
51
52
53
56
59
60
Halemaumau
250 meters

Graphs corresponding to the CO_2 flux at sites within Area F2.

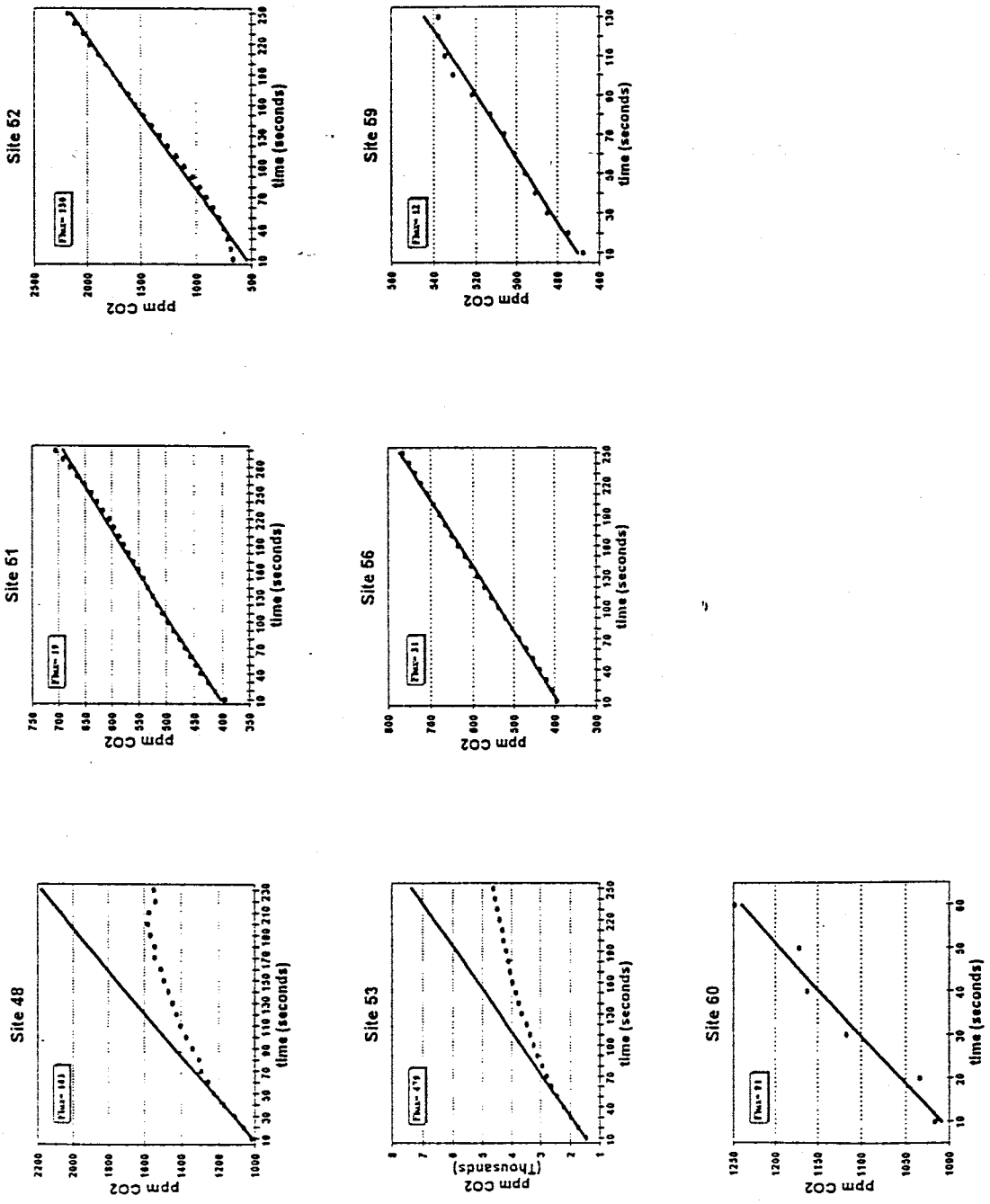

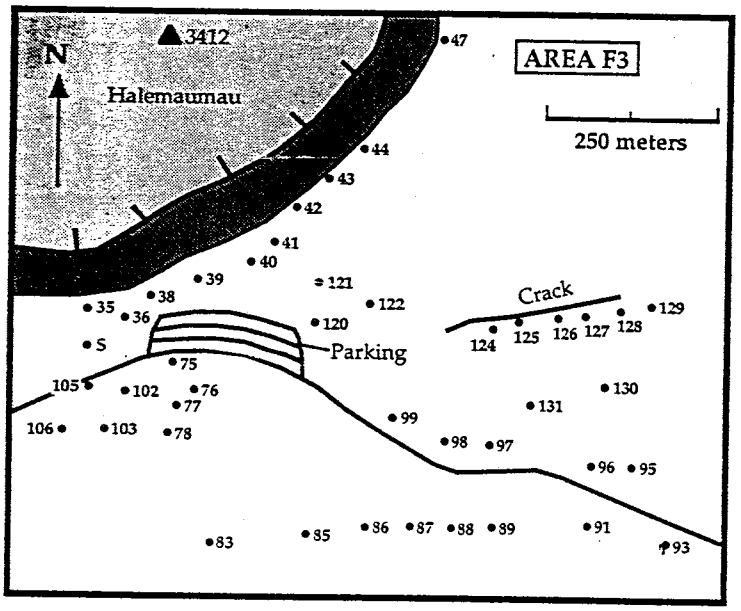
N
3412
Halemaumau
AREA F3
250 meters
47
44
43
42
41
40
39
38
121
122
35
36
120
Crack
129
124
125
126
127
128
S
Parking
75
105
102
76
77
130
131
106
103
78
99
98
97
96
95
83
85
86
87
88
89
91
93

Graphs corresponding to the CO_2 flux at sites within Area F3.

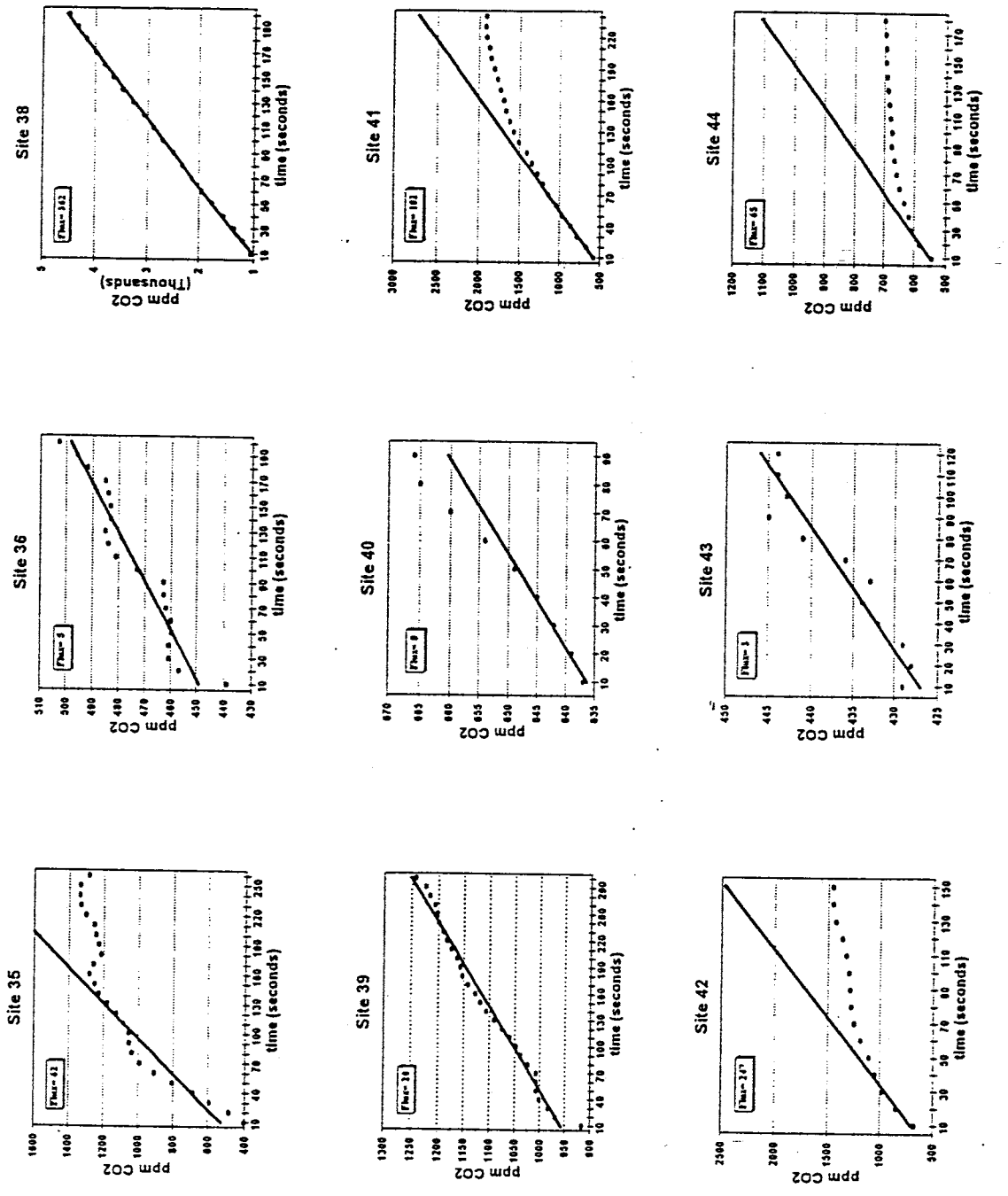

Graphs corresponding to the CO_2 flux at sites within Area F3.

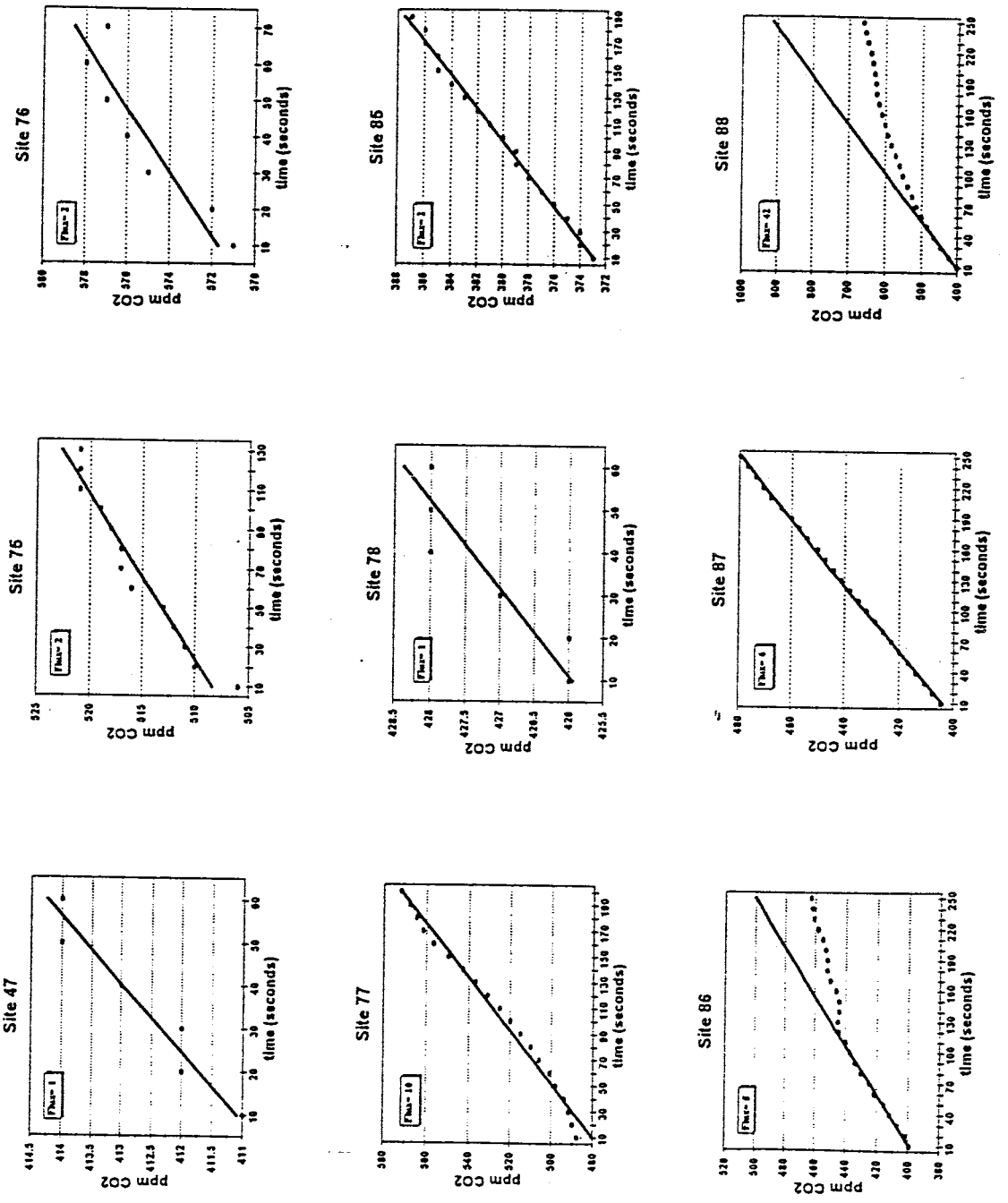

Graphs corresponding to the CO_2 flux at sites within Area F3.

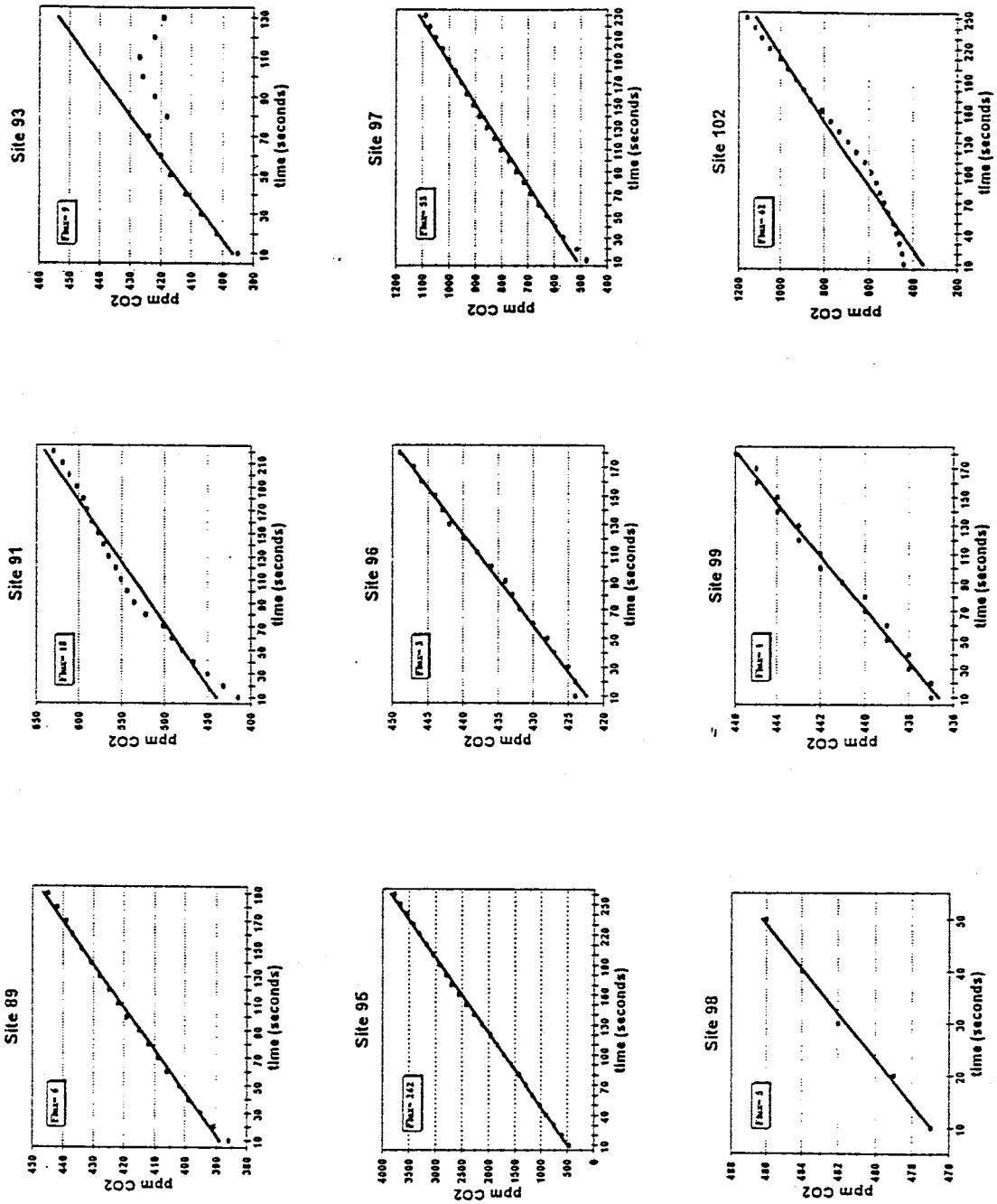

Graphs corresponding to the CO_2 flux at sites within Area F3.

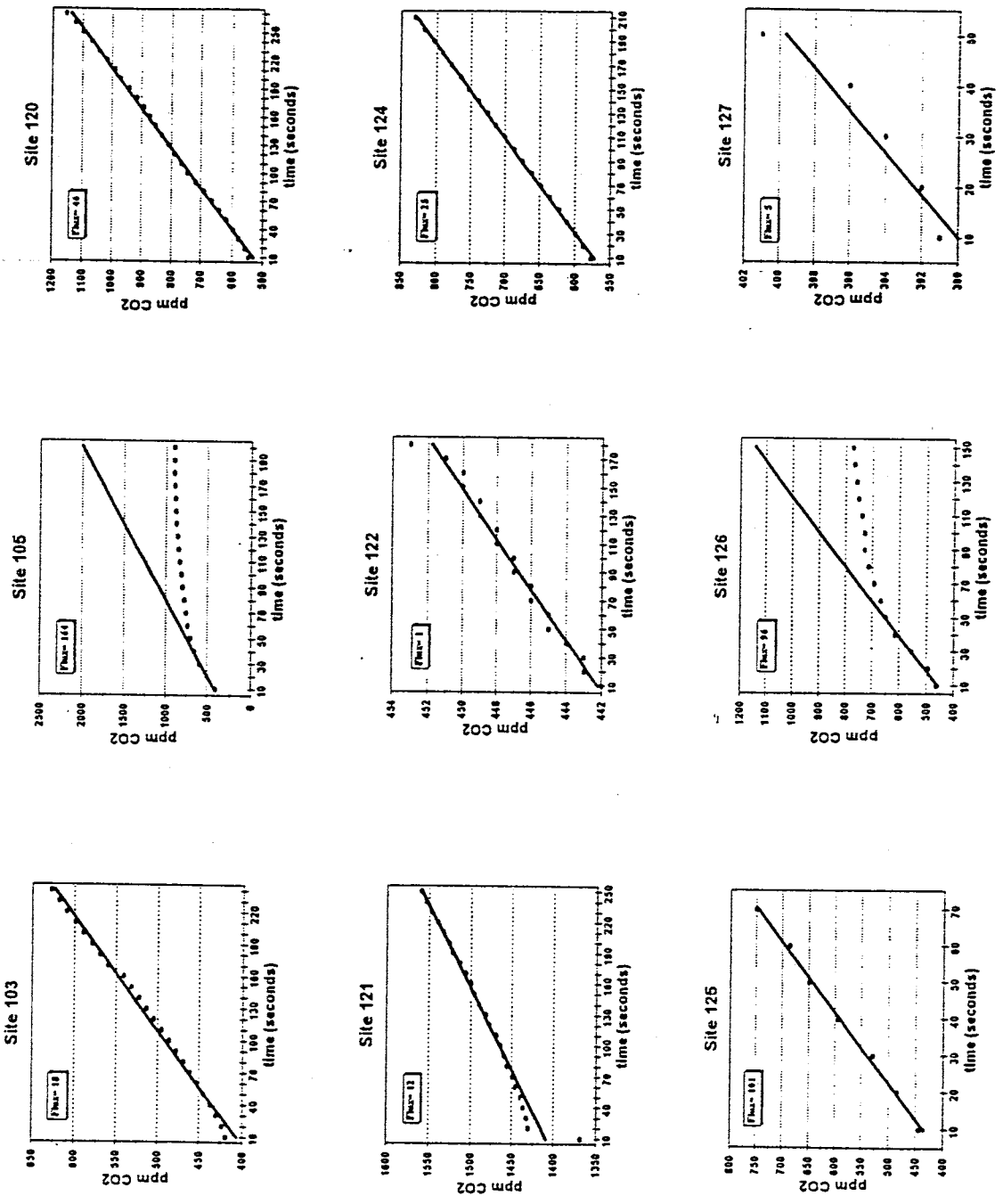

Graphs corresponding to the CO_2 flux at sites within Area F3.

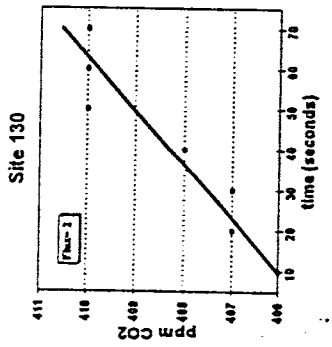

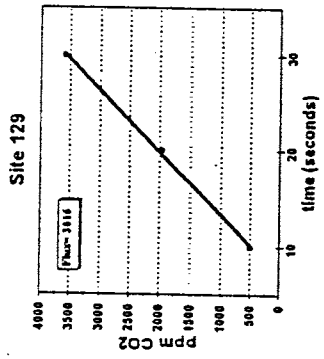

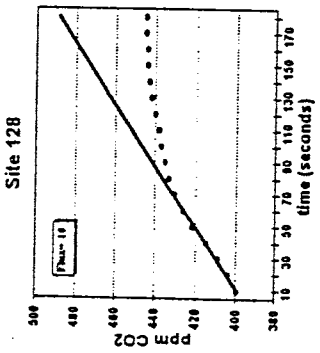

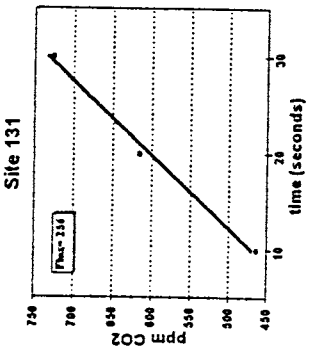

Graphs corresponding to the CO_2 flux at sites along Transects A through I.

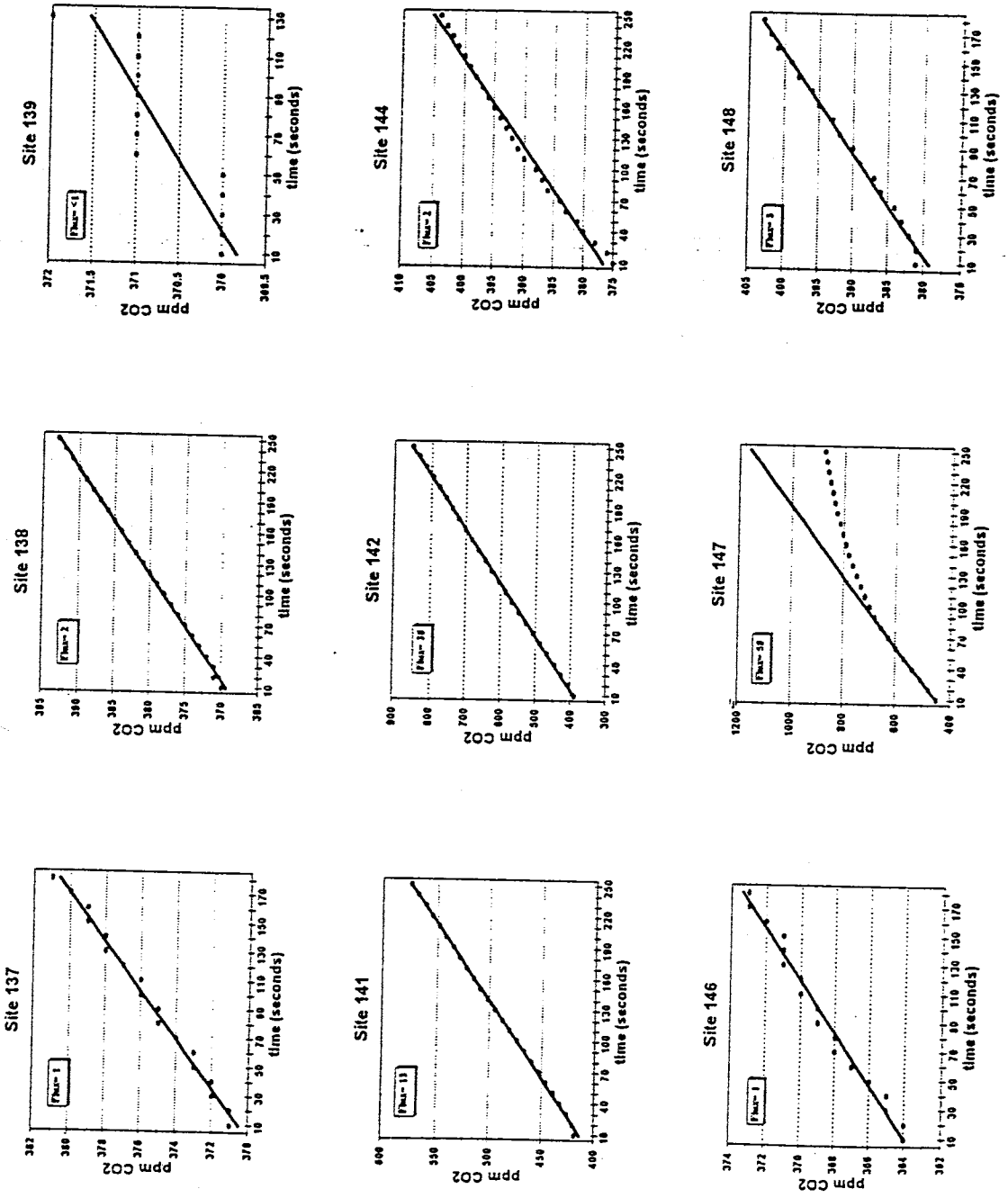

Graphs corresponding to the CO_2 flux at sites along Transects A through I.

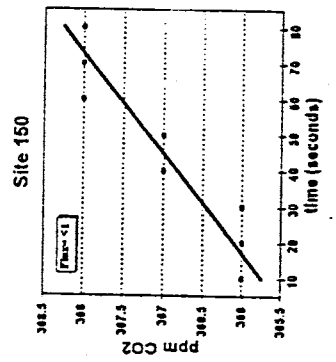

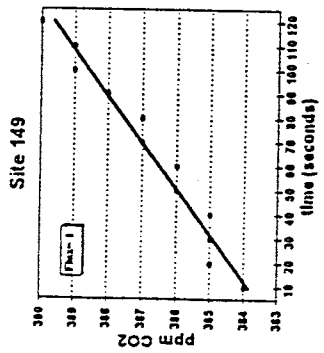

This thesis is accepted on behalf of the faculty of the Institute by the following committee:

David B. John for Philip Kyle
Adviser

Andrew Campbell

David B. John for Nelia Dunbar

Dec 5th, 1994
Date